Metal complexation, FT-IR characterization, and plankton abundance in the marine surface microlayer of coastal areas in the Eastern Mediterranean

Sotirios Karavoltsos[1]*, Aikaterini Sakellari[1]*, Marta Plavšić[2], Georgios Bekiaris[3], Dimitra Tagkouli[4], Anastasios Triantafyllidis[5], Antonia Giannakourou[5], Soultana Zervoudaki[5], Ioannis Gkikopoulos[1] and Nick Kalogeropoulos[4]

[1]Laboratory of Environmental Chemistry, Department of Chemistry, National and Kapodistrian University of Athens, Athens, Greece, [2]Ruđer Bošković Institute, Center for Marine and Environmental Research, Zagreb, Croatia, [3]Laboratory of General and Agricultural Microbiology, Agricultural University of Athens, Athens, Greece, [4]Department of Nutrition and Dietetics, School of Health Science and Education, Harokopio University of Athens, Athens, Greece, [5]Hellenic Centre for Marine Research HCMR, Institute of Oceanography, Attica, Greece

Barely any data exist on metal speciation in the marine surface microlayer (SML), a rather complex environment, the study of which contributes to enhancement of knowledge on metal speciation and its effect to the ocean. Metal speciation is significant since life requires a wide variety of trace metals that are essential for the growth of the organisms. Ligand concentrations (L) of copper (Cu), zinc (Zn), and cadmium (Cd) were studied by anodic stripping voltammetry (ASV) in the SML of coastal areas within the Aegean Sea in the Eastern Mediterranean. Complexing capacities in the SML in decreasing order ranged for Cu from 29 to 201 nM (median 101 nM), for Zn 24–149 nM (45 nM), and for Cd 1.0–1.5 nM (1.4 nM). Average enrichment factors (EFs) of SML samples compared to subsurface ones (SSW) were calculated equal to 0.9 ± 0.8, 1.2 ± 0.5, and 1.7 ± 1.6 for L_{Zn}, L_{Cu}, and L_{Cd}, respectively. In five out of the six total paired samples of SML and SSW, lower concentrations of L_{Zn} were measured in the SML, which is not the case for L_{Cu} and L_{Cd}. Due to elevated dissolved Zn concentrations in the SML, its complexation is incomplete, contrary to those of Cu and Cd, which are fully complexed. These trace metals are essential nutrients for biological functions, hence any differences on their concentration and chemical speciation may directly influence the distribution of phytoplankton species in the upper water column and neuston. EFs of SML relatively to subsurface water ranged in average between 1.2 and 2.4 for total organic carbon (TOC), chlorophyll a (Chl$a$), and plankton, being generally >2 for most of the amino acids detected, demonstrating a relative enrichment of the SML in organic matter. A significant correlation was found between Cu ligands and

dinoflagellates <20 μm, confirming older findings supporting that marine dinoflagellates of *Gymnodinium* genera produce Cu ligands. New insights are provided in the study and the importance of investigating bio-essential metal ions (Cu, Zn, Cd) and their organic complexes in the SML is pointed. Data on Zn and Cd complexing capacities in the SML are the first published so far.

Introduction

Dissolved metals [e.g., copper (Cu), iron (Fe), zinc (Zn), cadmium (Cd), lead (Pb), cobalt (Co)] are known to bind with available organic ligands in the ocean (Wells et al., 1998; Gledhill and Buck, 2012; Kim et al., 2015a; Noble et al., 2017; Zitoun et al., 2021). Their bioavailability and toxicity depend on their speciation (van den Berg and Donat, 1992; Wells et al., 1998; Santos-Echeandía et al., 2008), with their ionic and other labile forms (mainly inorganic complexes) being the most toxic for phytoplankton (Gachter and Mares, 1979), invertebrates (Andrew et al., 1977; Lorenzo et al., 2005), and fish (Davies et al., 1976), while their complexed ones (mainly with organic ligands) are noticeably less toxic. Several studies demonstrated the importance of metal–organic complexation in seawater, potentially affecting the metabolic processes of organisms such as phytoplankton and the marine biogeochemical cycles (Morel, 2008; Vraspir and Butler, 2009; Gledhill and Buck, 2012). The chemical nature of metal–ligand complexes and their wide size spectrum alter their kinetic inertness and potentially affect their bioavailability. As a bioactive element, Cu is complexed by dissolved organic ligands. Weaker organic ligands play a significant role in the reduction of Cu toxicity against phytoplankton growth, whereas other metals such as Fe tend to react with stronger ligands (Hirose, 2007). Similarly, at high concentrations, Zn could be toxic to phytoplankton and bacteria, but Zn concentrations in the surface seawater could be a limiting factor for phytoplankton growth (Sunda and Huntsman, 1998). In most surface waters, Zn is strongly bound with organic ligands, which results in reducing the fraction of free zinc ion (Zn^{2+}), which in low levels is necessary for the growth of some phytoplankton species (Sunda and Huntsman, 1995). Cd is also highly complexed by organic ligands in surface waters in comparison to the deep waters (Bruland, 1989), and organic ligands may play a role in attaining the benefits and hindering the toxic effects of the presence of this metal. Both Zn and Cd display a nutrient-like distribution profile in the ocean (Bruland, 1989; Bruland, 1992; Lee et al., 1995). Valuable pertinent information is obtained through the measurement of the complexing capacity of metal ions (*L*), denoting the capacity of water to reduce the toxic effects of metals through the formation of organic complexes (Hart, 1981), while some exceptions to this classical consideration show enhanced metal bioavailability in the presence of metal complexes (Zhao et al., 2016). Kim et al. (2016) concluded that the nature and concentration of ligands change over time and space and that our ability to quantify the effects of ligands on trace metal availability will be enhanced further by the development and validation of electrochemical techniques such as anodic stripping voltammetry (ASV) that provide an overall quantification of the bioavailability of the metals of interest. The specific method, which is well-established for more than 40 years, does however have some limitations due to several assumptions regarding, e.g., ligand classes' definition. Nevertheless, it is one of the analytical methods where no pretreatment of the samples is needed (e.g., for the removal of the high-salt matrix).

Speciation of the metal ions is affected by biologically produced organic ligands. Organic molecules could form complexes with metal ions due to the presence of different functional groups (e.g., -COOH, -OH, and -NH₂). In recent years, there has been remarkable progress toward the identification of feedback effects between metal ion speciation and the structure of planktonic microorganism communities. More than 40 iron-binding siderophore compounds from marine bacteria have been characterized (Vraspir and Butler, 2009), and some of them occur in ocean surface waters (Gledhill et al., 2004; Bundy et al., 2018). Porphyrins, the iron-binding molecules, are suggested to be released into seawater by cell lysis, passive excretion, or during zooplankton feeding (Witter et al., 2000; Vong et al., 2007). Humic substances of low molecular weight and thiols are Cu-binding compounds probably produced by picoplankton and coccolithophorids (Gordon et al., 1996; Laglera and van den Berg, 2003). Recently, Gledhill et al. (2022) working on iron chelates confirmed that binding site distributions in marine dissolved organic matter are heterogeneous and similar to those of humic substances.

Although the bulk of essential trace metals reaching the ocean through the atmosphere enter the surface waters through the surface microlayer (SML), little is known about the enrichment and interactions of these trace metals with organics in the SML (Cunliffe et al., 2013). The SML, a thin film-like layer, with approximately 50-µm thickness (Liss and Duce, 1997), is an extreme environment at the water–atmosphere interface characterized by high irradiation and temperature variability, where a high amount of organic material is concentrated (Wurl et al., 2017). It has been demonstrated that the sea surface is generally enriched in various elements and substances due to adsorption of surface-active substances (SASs) accumulated by gas bubbles arising from the subsurface layers (SSW) (Kuznetsova and Lee, 2002) and Langmuir circulations (Hardy, 1982). Among the various organics such as proteins, polysaccharides, and lipids that are present in the SML (Gašparović et al., 2007), it has been shown that lipids in particular play a substantial role in the formation of marine surface films (Brinis et al., 2004). It has been hypothesized that particle aggregation may be enhanced in the SML due to coagulation of the concentrated dissolved organic matter (Wurl et al., 2011). Various microorganisms utilize this organic matter directly, resulting in planktonic communities in the upper 5 cm of the water column that differ significantly from those in the SSW both in composition and abundance (Hardy, 1997). In addition, the intense UV (ultraviolet) irradiation in the surface waters, causes the quick photodecomposition of the produced fresh organic material. The differentiation of both the biology and the composition of organic matter between the SML and the subsurface water layers is likely to affect both qualitatively and quantitatively the metal ligands present.

The present study aims to determine the complexation capacities for Cu, Zn, and Cd ions employing an electrochemical technique [differential pulse anodic stripping voltammetry (DPASV)] combined with attenuated total reflectance Fourier transform infrared (ATR-FTIR) spectroscopy and gas chromatography/mass spectrometry (GC/MS) data on the chemical composition of organic ligands present in marine surface coastal samples. No data on Zn and Cd complexing capacities in SML have been published so far in the literature. On the contrary, there are available data for the speciation of Cu (Chen et al., 2006; Gašparović et al., 2007; Plavšić et al., 2007; Karavoltsos et al., 2015), which maintains a unique biological role, since even though it is essential for growth, it can be toxic at low concentrations (Posacka et al., 2019). Abundance and composition of plankton communities (ranging from picoplankton to mesozooplankton) were also studied, since they constitute the source of a significant amount of autochthonous organic matter. In coastal areas, the contribution of other sources of organic matter (i.e., allochthonous) is quite possible.

Materials and methods

Study area

Two coastal sites were studied within the Aegean Sea (Greece, Eastern Mediterranean), namely, Loutropyrgos in the gulf of Elefsis and Pahi of Megara situated outside the gulf, at its western entrance (Figure 1). Differing in terms of their topographical features (depth, occurrence of estuaries) and anthropogenic pressures, the two sites represent different microenvironments. Loutropyrgos site (15–20-m depth) is located close (approximately at a 3-km distance) to the industrial zone (the largest in Greece) of Elefsis Gulf, a relatively shallow embayment (maximum depth 33 m), characterized by a particularly slow water recirculation, enhancing pollution problems observed in the inner part of the gulf (Prifti et al., 2022). The bay is in contact with Saronicos Gulf through two narrow channels at its eastern and western parts. At the northeastern coastal part of Elefsis Gulf, a significant number of industrial activities occur, including among others shipyards, oil refineries, and cement and metallurgical industries (Scoullos, 1986). Pahi sampling station (30–50-m depth) is in direct contact with the open waters of Saronicos Gulf, located within the wider area of the Liquefied Natural Gas (LNG) terminal of Greece, installed on the small island Revithousa.

According to the results obtained from the 6-year monitoring of dissolved metal concentrations in coastal and transitional waters of Greece (Tzempelikou et al., 2021), the background upper limits (BAC) mainly of Cu, followed by Zn and Cd, were exceeded within the Gulf of Elefsis. Despite the great anthropogenic pressures and pollution occurring, the western part of the gulf is particularly productive, as reflected in the higher chlorophyll a (Chl$a$) levels measured at the area of Loutropyrgos in comparison to Pahi of the Megara site (Karavoltsos et al., 2015).

Sampling

Representative sampling of SML remains challenging, since a routine collection of the uppermost molecular layer at the air–water interface, remaining unaffected by the subsurface layers, is not feasible (Engel et al., 2017). Under this perspective, both the sampling method applied and ambient conditions prevailing (wind speed close to the sea surface and sea surface state) are significant in characterizing the formation level of SML. In the present work, all samples were obtained under calm weather conditions (wind speed <6 m s^{-1}; flat sea surface). During three sampling campaigns performed in February, May, and September 2018, single samples were collected from the SML and subsurface water at 20-cm (SSW$_{0.2}$) and 2-m (SSW$_2$) depth. The glass plate of
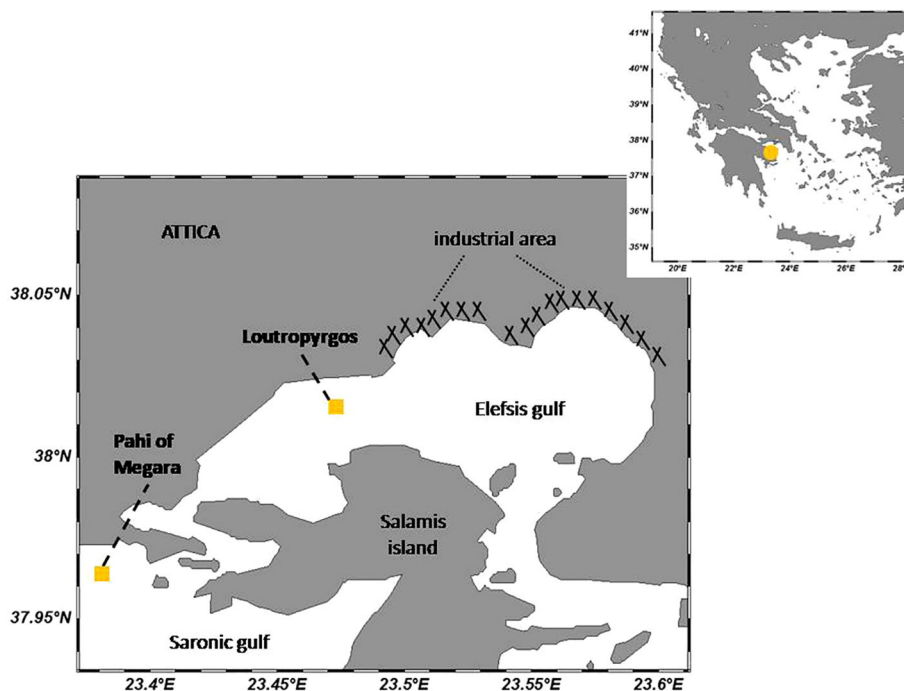
FIGURE 1
Coastal sampling sites (Schlitzer, Reiner, Ocean Data View, odv.awi.de, 2021).

Harvey and Burzell type (Harvey and Burzell, 1972) was used for the collection of the upper ~50 μm of SML, whereas SSW was manually collected in 2-L containers immersed at 20-cm depth and with a Nansen bottle from 2-m depth below the sea surface. Containers used for sample collection were thoroughly cleaned with detergent, rinsed with ultrapure water of 18.2 MΩ cm (Millipore, Bedford, MA, USA), filled with 10% nitric acid supra pure for several days, and subsequently rinsed with ultrapure water and seawater sample before sampling. Prior to its use, the glass plate was acid cleaned and rigorously rinsed with Milli-Q water, while sample collection started after the first five dips of the plate into seawater, for conditioning purposes. The potential contamination of sampling using the glass plate sampler was checked by rinsing the glass plate with ultrapure water, and the sample signal-to-blank ratio was generally higher than 5:1 for all metals. Sampling was carried out with the use of a small tender boat, equipped with an electric engine and remaining stationary during the sampling process. Samples were transported within a 4-h time frame refrigerated to the laboratory, where they were filtrated through 0.4-μm Whatman Nuclepore filters. For FTIR spectra, GF/F filters were used. Subsamples for total dissolved metal analysis following filtration were acidified with HNO_3 supra pure. The determination of TOC and SAS was completed within 24 h from sample collection, of L within 48 h, while of the other parameters in the next days. Physicochemical parameters (seawater temperature, pH, salinity) were measured *in situ* with

a YSI 63 pH/conductivity meter (YSI, Brannan Lane, OH, USA), equipped with an electrode frequently calibrated. Solar irradiation and air temperature were recorded with a DO9721 (probe LP9021) quantum photo-radiometer (Delta Ohm, Padova, Italy) and wind speed with a Testo 425 anemometer (Testo Inc., Sparta, NJ, USA). Seawater temperature, pH, and salinity were measured both at the upper 5 and 20 cm of the water column and at 2-m depth at each sampling station (Table 1).

Electrochemical analysis, metal concentration determination

Total dissolved Cu, Zn, and Cd concentrations were determined using the slightly modified rapid solvent extraction technique described by Danielsson et al. (1982). The procedure was carried out inside a clean room for minimizing the risk of metal contamination. Briefly, metal complexation in the seawater samples (200 mL) was performed by the addition of a combined complexing reagent of ammonium pyrrolidine dithiocarbamate and diethylammonium diethyldithiocarbamate (APDC/DDDC) at pH 4.5 ± 0.5. Carbamate-complexed metals were isolated by chloroform extraction and subsequently decomposed through acid addition (2 mL). Trace metal determination in the preconcentrated samples was performed by inductively coupled plasma mass spectrometry (ICP-MS) using a Thermo Scientific

TABLE 1   Sampling dates, environmental and physicochemical conditions.

Sample	Date	Sampling time (h)	Weather conditions	Solar irradiation (W m^{-2})	T_{air} (°C)	Wind Speed (m s^{-1})	T_{sea} (°C)	pH	Salinity (‰)
Loutropyrgos SML[a]	13.02.18	7:45 – 9:15	Sunny with light fog	24,000	14.5	1.3	13.8	7.85	38.2
Loutropyrgos SSW$_{0.2}$							13.7	7.84	38.3
Pahi SML		10:45 – 12:00	Sunny, partly cloudy	38,500	13.6	1.2	13.9	7.82	38.2
Pahi SSW$_{0.2}$							13.8	7.83	38.2
Loutropyrgos SML[a]	16.05.18	7:30 – 8:50	Sunny, partly cloudy	28,000	19.5	0.9	16.8	7.98	38.3
Loutropyrgos SSW$_{0.2}$							16.7	7.99	38.1
Loutropyrgos SSW$_2$							16.1	7.97	38.1
Pahi SML		10:00 – 12:30	Sunny, partly cloudy	45,000	22.0	0.5	17.0	7.96	38.6
Pahi SSW$_{0.2}$							16.8	8.00	38.5
Pahi SSW$_2$							16.6	7.99	38.4
Loutropyrgos SML[a]	05.09.18	9:00 – 10:30	Sunny	41,500	29.3	5.2	23.6	8.08	38.5
Loutropyrgos SSW$_{0.2}$							23.6	8.09	38.5
Loutropyrgos SSW$_2$							23.2	8.06	38.3
Pahi SML		13:00 – 14:30	Sunny	75,000	33.6	3.5	23.4	8.10	38.4
Pahi SSW$_{0.2}$							23.5	8.14	38.4
Pahi SSW$_2$							23.2	8.15	38.2

[a]Measurements of seawater temperature, pH and salinity were made in the upper 5 cm of the water column.
SML, surface microlayer; SSW$_{0.2}$, subsurface water at 0.2-m depth; SSW$_2$, subsurface water at 2-m depth.

ICAP Qc instrument (Waltham, MA, USA). Measurements were carried out in a single collision cell mode, with kinetic energy discrimination (KED) using pure helium (He). The limits of detection (LOD) of trace metals in sea water (nM) were equal to 0.003 for Cd, 0.1 for Cu, and 0.2 for Zn. The accuracy of the liquid extraction method applied was evaluated by the use of the certified reference material (CRM) "NASS-6, Seawater reference material for trace metals" (NRC-CNRC) (Table S1, Supplemental Material).

The electrochemical method of DPASV was used for complexing capacity determinations (Plavšić et al., 1982). Metal complexing capacity is the concentration of metal ions added to the seawater sample prior to their measurement as "free" metal ions (including hydrated metal ions and inorganic complexes, being labile for the applied electrochemical method and experimental conditions). The "inert complex" in terms of the DPASV method applied refers to the complex not dissociating under the chosen measurement timescale (stirring rate applied during the accumulation time). The quantity of the electro-inactivated metal is a measure of the amount of ligands (L) in the sample (Plavšić et al., 1982). The stirring rate during accumulation time in ASV defines the "detection window" of the ASV method. Davison (1978) pointed out that in ASV due to the possible kinetic effect, the "effective diffusion layer thickness" δ (the thickness of the layer formed in the vicinity of the electrode

surface), determined by the applied stirring rate, is the critical parameter. The thinner this layer is (at higher stirring rate), the smaller the number of complexes that will dissociate during deposition time.

Metal complexing capacity could be regarded as "metal ions buffering capacity." The strength of the organic complexes formed could be compared by their calculated apparent stability constant (K_{app}). The method of standard additions was implemented to the sample at its natural pH and to a sample aliquot acidified and UV irradiated. In order to minimize the effects onto the walls of the cell used for the measurements, the cell was rinsed in triplicate with approximately 10 mL of sample. After rinsing, 25 mL of the seawater sample was added to the cell. The equilibration time after each addition of metal was 15 min, which was proven to be adequate for the equilibration of metal ions studied, i.e., the peak height did not change after this period of time (Plavšić et al., 1982; Muller and Kester, 1991). The voltametric conditions were 300 s N_2 gas purge, 180 s deposition time for Cu, 200 s for Zn, and 120 s for Cd at -0.6 V deposition potential for Cu, -1.2 V for Zn, and -0.85 V for Cd. The apparent complexing capacity and the corresponding apparent stability constant were calculated by applying the linear transformation plot, assuming 1:1 metal-to-ligand complexes (Ružić, 1982; van den Berg, 1982). The slope

of this line determines the value of apparent complexing capacity (L) (slope = $1/L$), and the intercept on the y-axis determines the value of apparent stability constant (K_{app}) (intercept = $1/K_{app}L$).

SASs were determined by phase-selective alternating current voltammetry (PSACV) (Ćosović et al., 1985). Surfactant activity was expressed in terms of surfactant equivalents of the non-ionic surface-active compound Triton-X100 (MW ~600) in mg L^{-1}.

Electrochemical measurements were carried out using an Autolab III (Eco-Chemie, Netherlands) voltammetric instrument connected to a three-electrode cell (VA 663, Metrohm stand, Switzerland) with a static mercury drop electrode (SMDE) as the working electrode. The reference electrode was an Ag/AgCl (3 M KCl). A carbon rod electrode served as the auxiliary electrode. The methodology of electrochemical measurements applied is described in detail in Table S2.

Total organic carbon, transparent exopolymer particles, chlorophyll *a* determination

Total organic carbon (TOC) was determined by the method of high-temperature catalytic oxidation employing a TOC-5000A Shimadzu analyzer (Shimadzu Scientific Instruments, Columbia, MD, USA). The precision was estimated as the standard deviation (SD) between injections, and it was less than 2% of the mean. Concentrations of transparent exopolymer particles (TEPs) were measured according to the colorimetric method of Passow and Alldredge (1995).

For Chl*a* analysis, seawater samples (800 mL were passed through a Whatman GF/F filter (~0.7-μm pore size) and extracted overnight (16 h) in 10 mL of 90% acetone solution in the dark (Holm-Hansen et al., 1965). Chl*a* concentration was determined fluorometrically using a Turner 00-AU-10 fluorometer.

Fourier transform infrared spectroscopy

The FTIR spectra of the GF/F filters were recorded by a Spectrum Two FTIR spectrometer equipped with a Diamond ATR compartment (Perkin Elmer, USA) using the provided Spectrum 10 spectroscopy software. For each sample, 32 scans of the infrared region between 4,000 and 400 cm^{-1} at a resolution of 4 cm^{-1} were recorded in triplicate and averaged. The recorded spectra were then ATR-corrected with a refractive index of 1.5, smoothed by the Savitzky–Golay algorithm (total window of nine smoothing points and a zero-order polynomial), linearly baseline corrected and normalized by the mean using The Unscrambler 10.5 software (Camo, Norway).

Free amino acid, fatty acid, and sterol analysis

Following recording of suspended-matter FTIR spectra, filters were analyzed for free amino acids (FAAs), while samples from the survey of May were divided into two equal parts, one for FAA measurement and the other for fatty acid and sterol determination. The extraction of FAAs was performed according to Elmore et al. (2005) with minor modifications. For fatty acid and sterol analysis, half filters were extracted, subject to derivatization with BSTFA [N,O-Bis(trimethylsilyl) trifluoroacetamide] and analyzed by GC/MS (Agilent 6890N/ 5973). The methodology applied is described in detail in Table S2 (Supplemental Material).

Biological parameter analysis

Heterotrophic bacteria (HBA) and dinoflagellates (Dino) <20-μm counts were performed in 5–30-mL samples, fixed with borax-buffered formalin (final concentration 2% formaldehyde), filtered on black polycarbonate filters with 0.2- and 0.8-μm pore size (bacteria and Dino, respectively) and stained with DAPI (4′,6-diamidino-2-phenylindole) (Porter and Feig, 1980) using an epifluorescence microscope and UV–Blue excitation. For diatoms, Dino >20 μm and ciliate analysis, samples were fixed with Lugol's solution (acid for ciliates and Dino) and stored at 4°C until counting. For the analysis, 25–50-mL samples were left for 24 h for sedimentation and were then examined using an Olympus IX70 inverted microscope, equipped for phase contrast and image analysis, at 200× magnification. Cells were counted, distinguished into size classes and major taxonomic groups, and identified down to genus or species level where possible. Zooplankton samples were filtered through a 45-μm net, fixed with 4% buffered formalin, and analyzed using a stereoscope and image analysis PRO.

Statistical analysis

The t-test and Pearson correlations were carried out using the IBM SPSS software, version 28.0. A value of $p < 0.05$ (95% confidence level) was considered to indicate a significant difference (t-test, Pearson correlation). Principal component analysis (PCA) was performed on both the FTIR spectroscopic data and the amino acid profiles of the filters in order to detect a potential interrelation between the examined filters and their recorded ATR-FTIR spectra or their determined amino acid profiles. The analysis was performed by R-studio 1.0.136/R3.3.3 loaded with the "ade4" and "adegraphics" packages.

Results

In all samplings, the wind speed was <6 m s^{-1}, ensuring a well-organized SML. Water temperature and pH demonstrated typical seasonal variations. Surface water temperature is significantly affected by seasonal air temperature, as the bay is characterized by shallow depths with limited water renewal. Salinity slightly increased in surface layers (Table 1).

Differences between surface microlayer and subsurface waters

Suspended particulate matter

Suspended particulate matter (SPM) varied from 21.0 to 72.2 mg L^{-1} in SML and from 15.2 to 47.5 mg L^{-1} in subsurface layers (Table 2), being comparable to a previous work in the same area (Karavoltsos et al., 2015). In all sample pairs examined, the SML was found enriched in the SPM, with the enrichment factor (EF) of SPM (mean ± SD, 1.9 ± 1.0) significantly exceeding unity (t-test, $p = 0.043$), indicating enrichment, whereas in subsurface water layers at 20-cm and 2-m depth (SSW$_{0.2}$, SSW$_2$, respectively), SPM concentrations exhibited only small variations. The SML is typically enriched in suspended particulate matter, receiving particles that originate either from the atmosphere or from deeper waters (Cunliffe et al., 2013).

Metal concentrations and their ligands

Dissolved Zn, Cu, and Cd concentrations varied broadly (Figure 2; Table S3), exceeding those reported for open Mediterranean waters (Tovar-Sánchez et al., 2020), being however typical of coastal areas subject to intense anthropogenic pressures (Karavoltsos et al., 2021). Dissolved Zn and Cu concentrations were determined higher in SML compared to SSW, without any variations between samples obtained from 20-cm and 2-m depth (mean concentrations for Zn 23.2 ± 24.0 nM in SML, 9.2 ± 8.3 nM in SSW$_{0.2}$, 10.2 ± 8.7 nM in SSW$_2$; for Cu 18.8 ± 11.1 nM, 7.4 ± 4.4 nM, 7.4 ± 5.2 nM, respectively) (Figure 2; Table S3). The average enrichment factor of dissolved Zn in SML (EF = 2.4 ± 1.0), significantly exceeding unity ($p = 0.0027$), is slightly lower in comparison to the EF = 3.6 ± 3.0 reported for the period 2012–2013 for coastal areas in the Eastern Mediterranean (Karavoltsos et al., 2021). A relatively higher EF (9.4 ± 5.6) of dissolved Zn in SML has been previously calculated for the open waters of the Western Mediterranean (Tovar-Sánchez et al., 2020). The average EF of dissolved Cu in SML (2.6 ± 0.8), significantly higher than unity ($p = 0.0027$), is comparable to previous estimations (EF = 3.2 ± 2.6) reported for the same sampling stations (Karavoltsos et al., 2021). In the longitudinal section of western to eastern parts of the Mediterranean Sea, it was determined that SML is enriched in bioactive trace metal ions (i.e., Cd, Co, Cu, and Fe) with their levels being 8 (for Cd)- to 1,000 (for Fe)-fold higher than those of

TABLE 2 Suspended particulate matter (SPM), chlorophyll a Chla, total organic carbon (TOC), transparent exopolymer particle (TEP), surface-active substance (SAS) concentrations and their enrichment factors (EFs) in SML.

Sample*	SPM (mg L^{-1})	EF$_{SPM}$	Chla (mg L^{-1})	EF$_{Chla}$	TOC (mg L^{-1})	EF$_{TOC}$	SAS (mg L^{-1} T-X-100)	EF$_{SAS}$	TEP (µg Xeq L^{-1})	EF$_{TEP}$	SAS/ TOC
February 2018											
Loutr. SML	25.5	1.5	0.48	0.8	2.0	1.4	0.48	3.2	523	1.2	0.24
Loutrop. SSW$_{0.2}$	17.3		0.58		1.4		0.15		451		0.11
Pahi SML	21.0	1.1	0.32	6.4	2.4	1.5	0.54	3.4	830	2.5	0.22
Pahi SSW$_{0.2}$	19.8		0.05		1.6		0.16		326		0.10
May 2018											
Loutrop. SML	56.7	1.2	0.32	0.8	1.5	1.2	0.42	10.5	892	1.5	0.28
Loutrop. SSW$_{0.2}$	47.5		0.40		1.3		0.04		605		0.03
Loutrop. SSW$_2$	46.2		0.38		1.4		0.02		641		0.01
Pahi SML	55.4	1.4	0.21	3.5	2.0	1.2	0.35	5.8	788	2.5	0.18
Pahi SSW$_{0.2}$	39.7		0.06		1.7		0.06		310		0.04
Pahi SSW$_2$	38.8		0.06		1.5		0.06		274		0.04
September 2018											
Loutrop. SML	72.2	3.7	0.25	0.8	1.7	0.9	0.20	1.1	578	1.7	0.12
Loutrop. SSW$_{0.2}$	19.7		0.32		1.8		0.18		347		0.10
Loutrop. SSW$_2$	19.3		0.34		1.6		0.14		421		0.09
Pahi SML	34.9	2.3	0.06	0.8	1.9	1.1	0.12	1.3	607	1.1	0.06
Pahi SSW$_{0.2}$	15.2		0.08		1.7		0.09		552		0.05
Pahi SSW$_2$	18.3		0.08		1.7		0.11		510		0.06

*SML, surface microlayer; SSW$_{0.2}$, subsurface water at 0.2-m depth; SSW$_2$, subsurface water at 2-m depth.
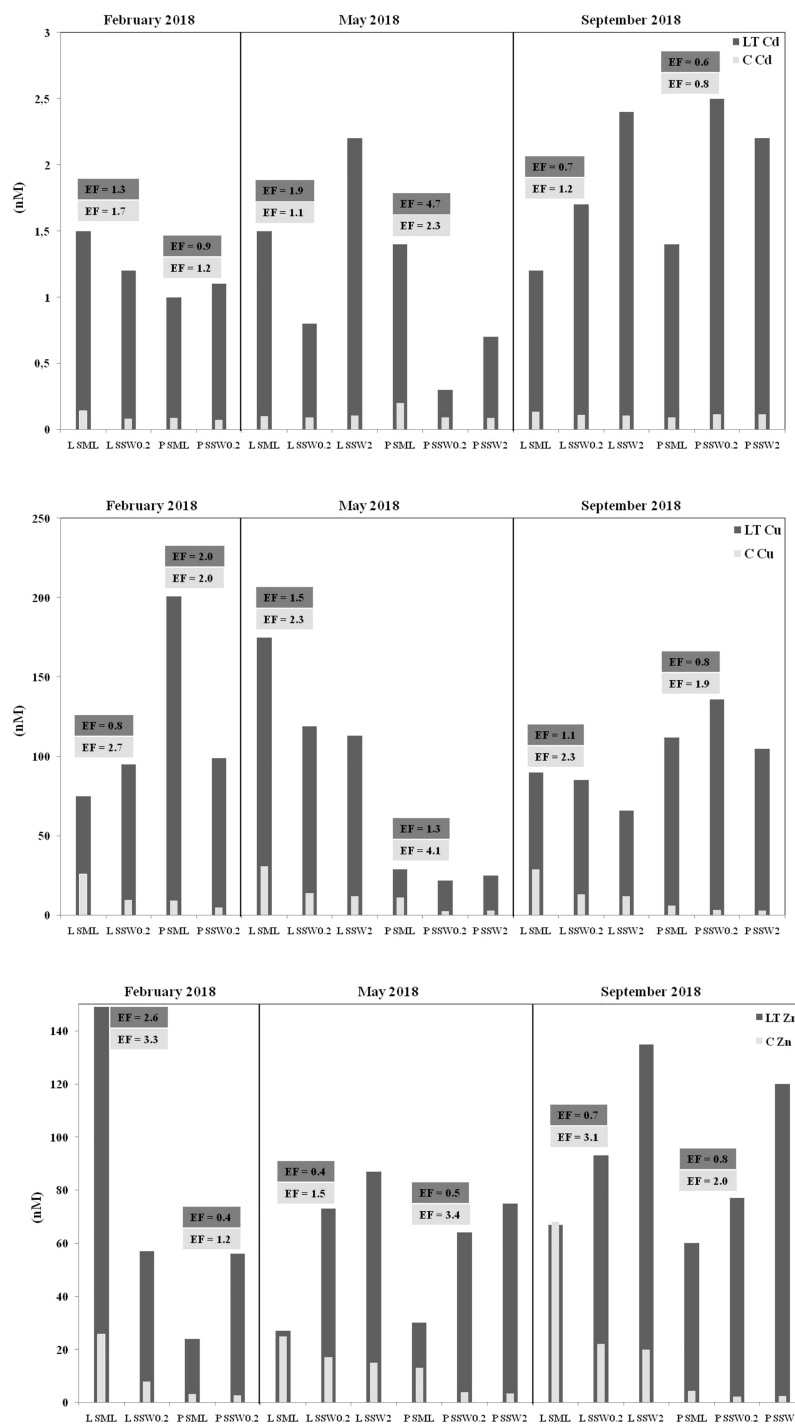
FIGURE 2
Metal-binding ligands (L_{Cd}, L_{Cu}, L_{Zn}), dissolved metal concentrations (C_{Cd}, C_{Cu}, C_{Zn}), and their enrichment factors (EFs) in surface microlayer (SML) and sub-surface (SSW$_{0.2}$, SSW$_2$) marine coastal waters of Loutropyrgos (L) and Pahi of Megara (P) sampling sites.

dissolved metal pools in the underlying water column (Tovar-Sánchez et al., 2014).

The average Zn-complexing capacity (L_{Zn}) gradually increased with depth (mean concentrations 60 ± 47 nM in SML, 70 ± 14 nM in $SSW_{0.2}$, 104 ± 28 nM in SSW_2) (Figure 2; Table S3). In most of the sample pairs examined (excluding Loutropyrgos in winter), L_{Zn} concentrations in SML were lower than those in SSW. On the contrary, L_{Cu} concentrations gradually decreased with depth (114 ± 64 nM, 93 ± 39 nM, 77 ± 40 nM, respectively); the enrichment factor of Cu ligands in the SML (mean EF = 1.3 ± 0.5) did not statistically significantly exceed unity (p = 0.120).

Homogeneity characterizes average dissolved Cd concentrations, both among different depths (0.125 ± 0.042 nM, 0.094 ± 0.017 nM, and 0.102 ± 0.012 nM in SML, $SSW_{0.2}$, and SSW_2, respectively), as well as among different sampling sites and seasons (Figure 2; Table S3). These findings reflected on the enrichment factor in SML (mean EF = 1.4 ± 0.5), not significantly differing from unity (p = 0.070). Similar levels of average Cd complexing capacity (L_{Cd}) were obtained at the various sampling depths examined (1.3 ± 0.2 nM, 1.3 ± 0.8 nM, and 1.9 ± 0.8 nM in SML, $SSW_{0.2}$, and SSW_2, respectively). No literature data concerning L_{Cd} and L_{Zn} in the SML are so far available.

The relative stability of metal complexes can be compared on the basis of their apparent stability constants ($\log K_{app}$). The determined $\log K_{app}$ values fall in the ranges 7.4–8.5 (Cu), 7.4–8.8 (Zn), and 8.7–9.9 (Cd). No difference of $\log K_{app}$ values was identified between SML and SSW samples, indicating the presence of metal ligands of similar nature among the different surface water layers (Table S3).

Chlorophyll a, total organic carbon, surface-active substances, transparent exopolymer particles

A Chl*a* SML enrichment was recorded only in two out of six sample pairs (Table 2), whereas the average EF in SML (2.2 ± 2.3) was not statistically significantly higher than unity (p = 0.13). These results confirm previous findings within the same area, including also the absence of significant enrichment of SML in Chl*a* (Karavoltsos et al., 2015).

The entire set of paired samples examined highlighted an enrichment of SML in TOC, SAS, and TEP (with the exception of TOC at Loutropyrgos site during September) (Table 2). The average EFs calculated decreased in the order SAS (4.2 ± 3.5), TEP (1.8 ± 0.6), and TOC (1.2 ± 0.2). According to the t-test applied, the mean EF was significantly greater than unity in the cases of SAS, TEP, and TOC (p = 0.038, p = 0.010, p = 0.028, respectively), denoting a statistically significant SML enrichment. In subsurface water layers (up to 2-m depth), TOC, SAS, and TEP concentrations appear uniform, presenting only small variations.

Amino acids, fatty acids, sterols

Eighteen amino acids were detected and quantified, namely, alanine, glycine, valine, leucine, isoleucine, threonine, serine, proline, asparagine, aspartic acid, glutamic acid, phenylalanine, glutamine, ornithine, lysine, histidine, tyrosine, and tryptophan. Among those, glutamic acid was the predominant one, in agreement with previous studies (Kuznetsova et al., 2004; Yang et al., 2009; Chen et al., 2013), followed by glutamine, lysine, ornithine, tryptophan, and tyrosine, with the majority previously reported in literature (Kuznetsova et al., 2004; Yang et al., 2009; Chen et al., 2013; How et al., 2014). Concentrations of FAAs ranged from 6.3 ± 1.8 to 31.0 ± 1.6 µg L^{-1} in SML samples, with glutamic acid, glutamine, lysine, ornithine, tryptophan, and tyrosine being the predominant ones, 2.4 ± 0.3 to 16.8 ± 1.6 µg L^{-1} in $SSW_{0.2}$ samples, with glutamine, glutamic acid, lysine, ornithine, tryptophan, and tyrosine being the most abundant, and 2.7 ± 0.5 to 11.8 ± 0.6 µg L^{-1} in SSW_2 samples, with glutamic acid, lysine, tryptophan, ornithine, tyrosine, and glutamine prevailing (Table S4; Supplemental Material).

Nine fatty acids, seven saturated and two unsaturated, were identified in Elefsis Gulf samples, with their total concentrations ranging from 16.4 to 78.2 µg L^{-1} (Table S5). SML was found enriched in total fatty acids compared to SSW at both Loutropyrgos (50.2 ± 2.0 µg L^{-1} in SML; 21.2 ± 6.8 to 23.7 ± 4.3 µg L^{-1} in SSW) and Pahi of Megara stations (77.7 ± 0.8 µg L^{-1} in SML; 27.4 ± 9.0 to 33.7 ± 0.6µg L^{-1} in SSW).

Total sterols ranged from 1.6 to 60.7 µg L^{-1}. The SML was enriched in individual and total sterols compared to SSW at both Loutropyrgos (4.5 ± 0.1 µg L^{-1} in SML; 1.9 ± 0.01 to 2.3 ± 0.1 µg L^{-1} in SSW) and Pahi of Megara stations (59.1 ± 2.3 µg L^{-1} in SML; 1.6 ± 0.01 to 2.2 ± 0.1 µg L^{-1} in SSW) (Table S6). Cholesterol (cholest-5-en-3beta-ol) and brassicasterol [(24/3)-24-methylcholesta-5,22E-dien-3/3-ol], which serve as ideal biomarkers of heterotrophic and autotrophic carbon pools, respectively, due to their abundance and environmental stability (Cavagna et al., 2013), were present in all samples examined (Table S6). Cholesterol is included among the predominant zooplankton sterols (Mühlebach et al., 1999), while brassicasterol, a phytosterol present in numerous algal classes (Volkman, 1986; Volkman, 2003), not biosynthesized by zooplankton, is commonly used as an indicator of marine algae, diatoms in particular (Cavagna et al., 2013). Serving as a tracer of sewage pollution due to its source specificity and environmental stability (Peng et al., 2005; Frena et al., 2016), coprostanol was not detected in any of the samples measured (Table S6). Known as markers of algae, Dino, diatoms, bacteria, and vascular plants input to surface waters (Volkman et al., 1998; Peng et al., 2005), sitosterol, stigmasterol, and campesterol were present in all examined samples. Cholesterol and sitosterol predominated in SML, while cholesterol and brassicasterol predominated in SSW layers.

Biological parameter abundance

Table 3 shows data for the abundance of bacterioplankton, diatoms, Dino <20 µm, Dino >20 µm, ciliates, and zooplankton at the two sampling sites examined. The abundance of all biological parameters was generally higher in SML compared to SSW, with average enrichment factors ranging from 1.5 to 2.4. However, no statistically significant SML enrichment (EF greater than unity) was obtained for HBA (EF = 1.5 ± 0.7, p = 0.061), ciliates (2.4 ± 3.0, 0.157), diatoms (2.0 ± 1.5, 0.078), Dino <20 µm (1.5 ± 0.8, 0.104), and Dino >20 µm (1.5 ± 0.5, 0.117) due to their broad abundance.

Differences among seasons and sites

The seasonal variation of dissolved Zn, characterized by higher concentrations in summer and lower ones in winter, is in accordance with previous findings for the same area (Sakellari, 2006). Within the gulf of Elefsis, where Loutropyrgos site is located, a thermocline prevails in the water column during the summer period. Its breakdown upon lowering of surface water temperature leads to water column mixing and water homogenization. During the thermocline formation, accumulation of Zn on the sea surface due to atmospheric deposition is reflected by increased Zn concentrations in surface waters, albeit the enrichment of deeper water layers,

attributed to a potential Zn flux at the sediment–water interface, calculated at Loutropyrgos equal to 0.8 mmol m^{-2} d^{-1} (Sakellari et al., 2011). Similarly, in Vigo Ria (NW Iberian Peninsula) characterized by a significant anthropogenic influence due to intense population presence and industry settled on its margins, benthic fluxes of dissolved trace metals were significant for most of the examined metals [Zn, Cu, nickel (Ni), vanadium (V)] (Santos-Echeandia et al., 2009). Dissolved Cd follows a uniform spatial and temporal distribution, confirming earlier measurements at the same area (Scoullos et al., 2006). Between the two areas studied, higher concentrations were found for dissolved Zn (up to 8-fold) and Cu (up to 5-fold) at Loutropyrgos site compared with the corresponding obtained for Pahi of Megara station, located outside the Elefsis Gulf, in direct contact with the open sea. In Elefsis Bay, characterized by intense industrial activity, dissolved Cu concentration is considered elevated, exceeding the background assessment concentration (BAC) for coastal marine waters in Greece (Tzempelikou et al., 2021). An increase in Zn ions complexing capacity with depth was observed during spring and summer at both sampling stations. During spring, in all depths (including SML), significantly lower L_{Cu} concentrations were determined at Pahi of Megara site in comparison to Loutropyrgos site (even 5-fold).

Seasonally, higher Chl$a$ levels were measured in February, when the characteristic annual phytoplankton bloom is observed

TABLE 3 Biological parameter abundance (cells L^{-1}, except for bacteria expressed as ×10^6 HBA mL^{-1} and zooplankton expressed as ind. m^{-3}) and their enrichment factors (EFs) in the marine surface microlayer.

Sample*	HBA	EF$_{HBA}$	Cilia.	EF$_{Cilia}$	Diatoms	EF$_{Diatoms}$	Dino <20 µm	EF$_{Dino<20µm}$	Dino >20 µm	EF$_{Dino>20µm}$	Zooplank.	EF$_{Zoopl.}$
February 2018												
LSML	3.30	1.9	1,360	1.7	175,605	0.7	4,674	1.5	6,240	1.4	-	-
LSSW$_{0.2}$	1.75		800		241,058		3,109		4,440		-	
PSML	1.16	1.0	480	2.4	81,562	4.6	5,258	1.4	840	2.8	-	-
PSSW$_{0.2}$	1.20		200		17,840		3,834		300		-	
May 2018												
LSML	1.65	1.1	440	0.2	102,418	2.8	6,846	0.7	8,480	1.0	381	-
LSSW$_{0.2}$	1.50		2,520		36,328		9,858		8,960		-	
LSSW$_2$	1.27		660		209,288		10,061		3,080		-	
PSML	0.62	0.8	220	1.0	174,197	1.7	3,834	1.4	2,480	2.1	1,043	-
PSSW$_{0.2}$	0.73		220		104,226		2,738		1,180		-	
PSSW$_2$	1.25		260		13,760		1,917		980		-	
September 2018												
LSML	2.45	1.7	1,240	0.5	109,635	1.0	8,505	3.1	3,760	1.0	1,249	10.5
LSSW$_{0.2}$	1.46		2,680		105,728		2,738		3,600		118	
LSSW$_2$	1.27		1,600		102,032		2,465		3,500		-	
PSML	2.87	2.6	6,220	8.2	332,467	1.2	9,311	0.9	3,120	0.5	696	1.6
PSSW$_{0.2}$	1.09		760		288,230		9,858		5,880		433	
PSSW$_2$	0.98		440		315,613		5,203		3,640		-	

*L, Loutropyrgos station; P, Pahi of Megara station; SML, surface microlayer; SSW$_{0.2}$, subsurface water at 0.2-m depth; SSW$_2$, subsurface water at 2-m depth; HBA, heterotrophic bacteria; Dino, dinoflagellates; ind., individuals.

by the end of winter. Among the areas studied, Loutropyrgos, within the gulf of Elefsis, is the most productive. In terms of seasonal variations, winter SML samples presented the highest amino acid concentrations followed by summer and spring ones. During winter, glutamic acid predominated, followed by glutamine, lysine, ornithine, tryptophan, and tyrosine, while in summer samples, the most abundant amino acids were glutamine, glutamic acid, lysine, ornithine, tryptophan, and tyrosine. In both cases, samples obtained from Loutropyrgos site contained higher amounts of amino acids compared to those from Pahi of Megara site. During spring, several amino acids were either present at very low concentrations or even non-detectable, with glutamic acid, proline, and alanine predominating and their highest concentrations being measured at Pahi of Megara site.

FTIR spectra revealed an intense variability of both absorption intensity (quantitative differences) and characteristic peak positions (qualitative differences) among the different sampling sites and sampling periods. Absorption peaks were observed at 3,350, 2,980, 2,890, 1,640, 1,425, 1,045, and 870 cm^{-1} (Figure 3A). The former peak is related to organic O-H and N-H group vibrations, while the peaks at 2,980 and 2,890 cm^{-1} were related to the asymmetric CH_3 and CH_2 stretching, respectively (Socrates, 2001). According to Tremblay and Alaoui (2011), these regions are more intense in particulate organic carbon (POM)-rich particles, while for peaks at higher wavenumbers (e.g., 2,980 cm^{-1}), the particles appear more aliphatic. The peak at 1,645 cm^{-1} corresponds to C=O stretching vibration attributed to amide I region, while the peak at 1,425 cm^{-1} is correlated to the deformation vibrations of aliphatic groups (Socrates, 2001; Tremblay and Alaoui, 2011). Finally, the peaks at 1,045 and 870 cm^{-1} are attributed to C-O stretching vibrations of carbohydrates and to C-H deformation vibration of pyranose compounds (Socrates, 2001). However, a peak shifting and new characteristic peaks were observed among the different sampling periods and sites (Figure 3). For water samples collected during winter (Figure 3B), the recorded spectra revealed a high aliphatic character of POM of samples collected from Loutropyrgos site, with peaks of very high intensity at 2,980, 2,904, and 1,420 cm^{-1}, while Pahi of Megara samples had a higher intensity at the carbohydrate region. This could be related with the higher sugar content of Pahi surface waters (Tremblay and Alaoui, 2011). However, Pahi of Megara samples collected during spring revealed a much higher aliphatic nature of POM particles, with strong peaks at 2,930, 2,860, and 1,432 cm^{-1}, presenting also a higher N content (~3,360 cm^{-1}) compared to the rest of the samples collected in different periods of the year. The lower SML carbohydrate content (1,052 cm^{-1}) was measured in spring samples, while the highest carbohydrate content was recorded during summer at both sampling sites (Figure 3D).

The highest bacterial abundance was found in SML of Loutropyrgos station during winter and the lowest in Pahi SML during summer (Table 3). The highest ciliate abundance was observed in Pahi SML during summer, whereas the lowest was observed in Pahi SSW during winter (6,220 cells L^{-1} and 200 cells L^{-1}, respectively). At Pahi station, the SML was enriched in diatoms compared to underlying and deeper waters. Diatom abundance peaked in Pahi SML during summer (332,467 cells L^{-1}). At both stations, Dino <20 μm and Dino >20 μm abundance were higher in SML compared to SSW during winter.

Discussion

Prevalence of ligands

Metal binding ligand concentrations decreased in the order Cu > Zn > Cd, while dissolved metal concentrations decreased in the order Zn > Cu > Cd. The same decreasing orders of Zn, Cu, and Cd ligands and dissolved metal concentrations were reported by Wells et al. (1998) in Narragansett Bay, in one of the limited studies simultaneously examining the speciation of the specific metals. Wells et al. (1998) also pointed out that despite the high degree of metal complexation, total ligand concentrations did not vary in accordance with dissolved metal concentrations.

Seasonal variations of L_{Zn} revealed a depletion of Zn ligands in SML compared to subsurface waters. This depletion relates with either the formation of a gelatinous layer within the SML through aggregation of organic molecules and the subsequent removal of Zn organic ligands in suspended matter or/and the rapid transformation of fresh organic material due to bacterial activity. At Narragansett Bay, Muller and Kester (1991) measured Zn complexing capacity ranging from 46 to 104 nM, whereas in open sea waters, particularly low L_{Zn} values are usually determined (Kim et al., 2015b). In near surface waters of subarctic North Pacific and Bering Sea, dissolved Zn speciation was dominated by the complexation to strong organic ligands, the concentrations of which ranged from 1.1 to 3.6 nM, with $\log K_{app}$ values varying from 9.3 to 11 (Jakuba et al., 2012).

Copper ligand enrichment factor in the SML (mean EF = 1.3 ± 0.5) was not significantly greater than unity (p = 0.120). Gašparović et al. (2007) reported a Cu complexing capacity of SML in the subarctic Norwegian fjords region varying from 230 to 1,790 nM, with an average enrichment factor of 2.5, while Plavšić et al. (2007) reported L_{Cu} values from 280 to 940 nM in the NW Mediterranean region, with an EF of 1.2, similarly to our previous work in coastal areas of the Eastern Mediterranean (EF = 1.2; Karavoltsos et al., 2015). Analytical methodologies with an identical "detection window" were applied in all aforementioned studies. In Jiaozhou Bay (a natural inlet of the Yellow Sea in China), the average EF of L_{Cu} in SML was recorded at 1.56 (Chen et al., 2006). Homogeneous spatial and temporal concentrations of Cd ligands were obtained in accordance to the findings of Wells et al. (1998), who demonstrated

that the Cd binding ligand concentration in Narragansett Bay remained essentially constant.

Characterization of organics, importance of phytoplankton

Ratios of surface-active substances/total organic carbon and transparent exopolymer particles *vs*. chlorophyll *a*

Valuable information on the characteristics of organic matter present in seawater is obtained by the normalization of surfactant activity (concentration of SAS) in terms of TOC concentration (SAS/TOC) measured in the same samples (Ćosović and Vojvodić, 1998; Gašparović et al., 2007). Higher SAS/TOC ratios indicate a greater contribution of hydrophobic substances to the organic matter pool, such as nonionic surfactants and lipids, while a lower SAS/TOC ratio indicates the presence and contribution of organic matter of a more hydrophilic type such as fulvic/humic acids, amino acids, and polysaccharides (Plavšić et al., 2007). All of the normalized surfactant activity values calculated in this study fall in the range 0.06–0.28 for SML, 0.03–0.11 for $SSW_{0.2}$, and 0.01–0.09

for SSW_2 samples (Table 2). SAS/TOC ratios obtained for SML and corresponding SSW samples denote an enrichment in hydrophilic compounds such as polysaccharides, with several SML samples differentiating, by demonstrating relatively higher SAS/TOC ratios (in particular during winter and spring) (Figure 4). Although different SAS types contribute to the surfactant activity of both SML and SSW, similar SAS/TOC ratios were obtained for SSW samples at 0.2- and 2.0-m depth, indicating a similar SAS type.

TEP and Chl*a* concentrations are significantly correlated during the exponential growth phase of phytoplankton batch cultures (Passow, 2002). The empirical equation TEP = a (Chl-$a)^b$ is considered as the best fit between TEP and Chl*a*. The exponent b represents the slope of linear regression under TEP and Chl*a* log transformation. Values of b are generally <1, supporting the hypothesis that TEP formation is a function of the phytoplankton growth rate rather than the standing stock (Passow, 2002, and references therein). A b value equal to 0.18 was calculated herewith, with a low linear correlation factor (r^2 = 0.20; n = 16). These findings comply with the consideration that the relation between TEP and Chl*a* is specific for each individual bloom, but no overall relationship between TEP and Chl*a* can be derived, since many other processes also interfere (Passow, 2002,
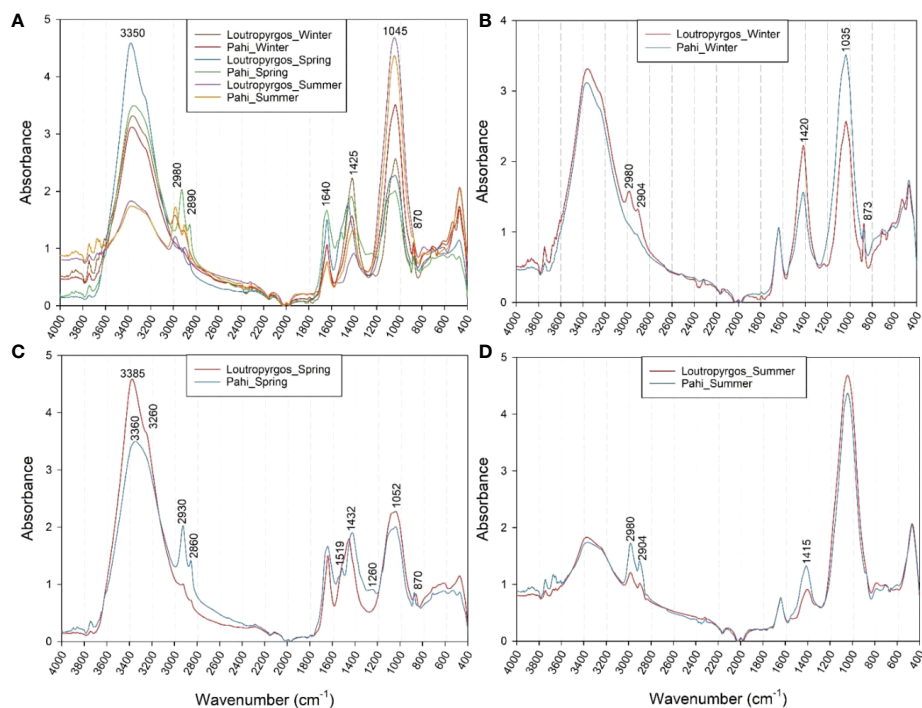

FIGURE 3
ATR-FTIR spectra of **(A)** all SML water samples collected from both sites, and their comparison according to the sampling period, i.e., during **(B)** winter, **(C)** spring and **(D)** summer.

and references therein). In a previous study for coastal SML samples originating from the same area, a b value equal to 0.12 ($r^2 = 0.01$; n = 27) was calculated (Karavoltsos et al., 2015).

Organic matter and attenuated total reflectance fourier transform infrared spectra

A principal component analysis (PCA) was performed on the recorded ATR-FTIR spectra of the samples analyzed in order to identify any grouping of the samples on the basis of 1) sampling depth (SML, SSW), 2) sampling season (summer, spring, winter), and 3) sampling location (Loutropyrgos, Pahi of Megara). The projection of first and second principal components (PC1 and PC2) allowed for a discrimination (across the PC2 axis) of the recorded spectra of SML samples, however not of the subsurface ones (Figure 5A). The interpretation of PC2 loadings (Figure 5B) revealed a positive correlation of surface water samples (negative loadings) with the spectral regions at 2,920 (aliphatic asymmetric C-H stretching), 1,660 (asymmetric NO_2 stretching in nitro compounds and organic nitrates, C=C stretching), 1,600 (C=C stretching), 1,509 (N-H stretching of amide II band, aromatic ring vibration, asymmetric NO_2 stretching in nitro compounds and organic nitrates), 1,415 (CH_3/CH_2 deformation vibrations), and 1,256 cm^{-1} (symmetric NO_2 stretching in organic nitrates, CH_2 wagging vibration, P=O stretching in phosphates) (Socrates, 2001). The projection of first and second principal components (PC1 *vs*. PC2, explaining 97% of variance) allowed for a clear separation (across PC1 axis) of the spectra in clusters, according to different sampling seasons (Figure 6A). The observation of the loadings for PC1 (Figure 6B) revealed a positive correlation of the samples collected during spring and winter with spectral regions at 3,360 (amines N-H stretching

vibrations), 2,924 (aliphatic asymmetric C-H stretching), 2,844 (aliphatic symmetric C-H stretching), 1,639 (alkenes C=C stretching), 1,504 (N-H stretching of amide II band, aromatic ring vibration, asymmetric NO_2 stretching in nitro compounds and nitrates), 1,445 (asymmetric C-H deformation), and 621 cm^{-1} (asymmetric NO_2 stretching in nitro compounds and nitrates) (Socrates, 2001). Samples collected during summer and possessing a positive correlation (negative loadings) with the spectral regions at 1,048 (C-O stretching vibration) and 800 cm^{-1} are assigned to several vibration/compounds such as N-H wagging in secondary amides, CH_2 rocking, or C-S stretching. In terms of sampling location, separation of the recorded spectra between the two sampling stations was not possible, indicating small differences in the samples' composition.

Free amino acid, fatty acid, and sterol distribution

FAAs are of great interest in oceanic and coastal waters, representing a good nitrogen source for marine microalgae and bacteria (Tada et al., 1998). A pattern similar to the PCA performed to FTIR spectra was obtained for amino acids, dividing the water samples in terms of seasonality across PC2 axis (Figure 7A) and depth across PC1 axis (Figure 7B). The calculated loadings, i.e., principal amino acids in each group (Figure 7C), revealed significant correlations between glutamic acid (Glu) and glutamine (Gln) in SML, among lysine (Lys), ornithine (Orn), tryptophan (Trp), glutamine (Gln), and tyrosine (Tyr) in summer and winter, and between proline (Pro) and glutamic acid (Glu) in spring.

Fatty acids are abundant in most aquatic environments, deriving from sources including bacteria, microalgae, higher plants, and marine fauna. Saturated fatty acids (SFAs) such as
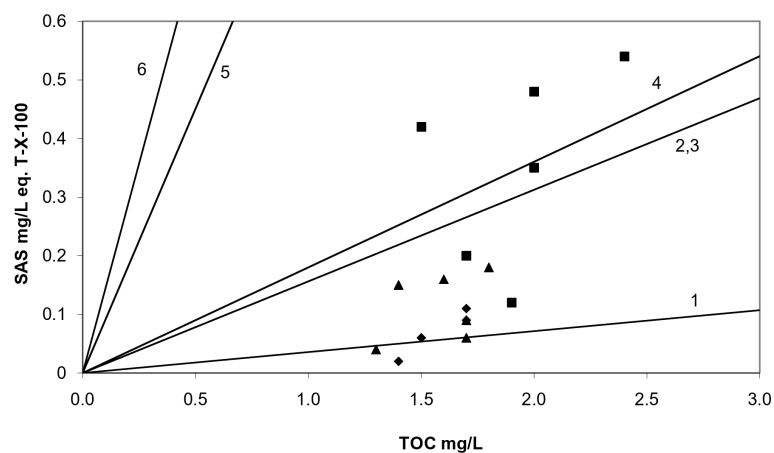

FIGURE 4
Correlation of SAS and TOC concentrations obtained in SML (□), SSW$_{0.2}$ (O), and SSW$_2$ (◇) seawater samples. Lines correspond to different model substances: no. 1 microbial polysaccharide xanthan, no. 2 protein (Albumin), no. 3 fulvic acid, no. 4 polysaccharide dextran T-500, no. 5 Triton-X-100, and no. 6 oleic acid. SML, surface microlayer; SSW$_{02}$, subsurface water at 0.2-m depth; SSW$_2$, subsurface water at 2-m.
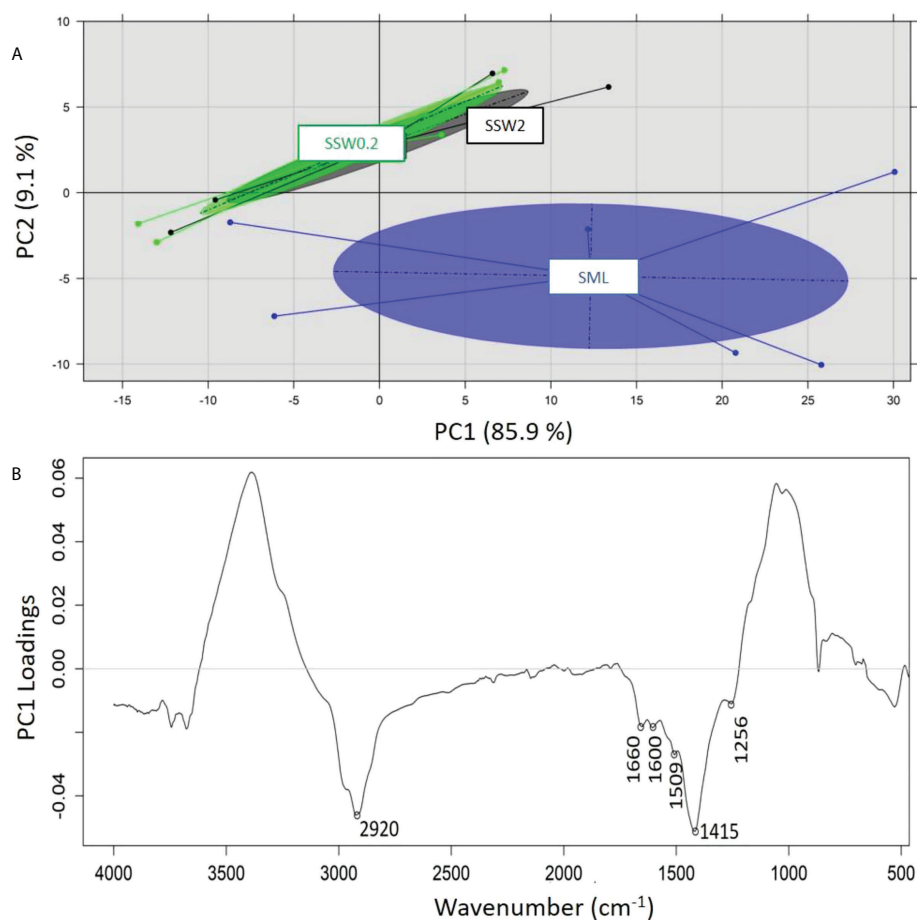
FIGURE 5
(A) Principal component analysis of recorded ATR-FTIR spectra and separation on the basis of sampling depth and **(B)** loadings of PC2 across which separation is realized.

palmitic and stearic (16:0 and 18:0, respectively) are ubiquitous. In Elefsis Gulf samples, SFAs predominated, comprising 78.2%–94.3% of total fatty acids, followed by monounsaturated fatty acids (MUFAs) accounting for 1.5%–10.3% and polyunsaturated fatty acids (PUFAs) accounting for 1.0%–19.9%. The lability and susceptibility of unsaturated fatty acids to oxidation (Gašparović et al., 2007) explain both their relatively low percentages within the Elefsis Gulf, as well as SML depletion observed in the Western Mediterranean (Saliot et al., 1991) and Norwegian fjords (Gašparović et al., 2007), whereas simultaneous predominance of SFAs was also reported. In accordance with previous findings for the Mediterranean (Goutx and Saliot, 1980; Saliot et al., 1991), palmitic acid (16:0) prevailed among the fatty acids determined in the suspended particulate matter of Elefsis Gulf, followed by stearic (18:0), oleic (18:1), and myristic (14:0) acids. At both stations, the SML was enriched in fatty acids, with enrichment factors exceeding 2 for total and the majority of individual fatty acids.

Sterols have been used to characterize the origin of particulate organic matter (Alsalahi et al., 2015). Employing sterols ratios in tracing the origin of particulate organic matter, sitosterol/campesterol ratio was applied in the SW Mediterranean (Dachs et al., 1998) and the mouth of Rhône River (Galeron et al., 2015). Ratios exceeding 1 indicate dominance of terrigenous particulate organic matter sources, whereas ratios lower than 1, organic matter of aquatic origin (Dachs et al., 1998). In the Gulf of Elefsis, sitosterol/campesterol ratios ranged between 3 and 12.6, pointing to a terrigenous origin of organic matter, complying with the semi-enclosed features of the area.

Sources of metal ligands

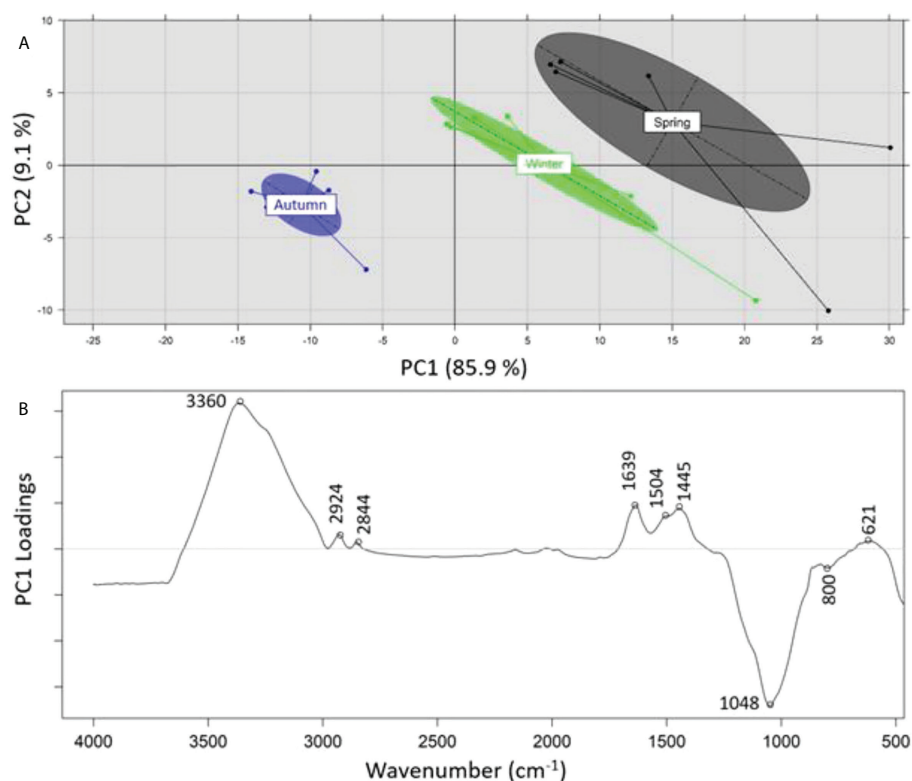Sources of metal ligands comprise substances deriving from phytoplankton, bacteria, coastal sediments, pore water, and

FIGURE 6
(A) Principal component analysis of recorded ATR-FTIR spectra and separation on the basis of sampling period, **(B)** loadings of PC1 across which separation is realized.

more inert humic substances (Kim et al., 2015b, and references therein). No correlation was observed between Chl$a$ and metal L_T, despite previous observations on phytoplankton blooms and laboratory cultures (Passow, 2002), whereas L_{Cu} and TEP correlated significantly (Pearson r = 0.63, p = 0.08, n = 16). During a *Navicula* sp. bloom at Loutropyrgos site (within the Gulf of Elefsis), Scoullos et al. (2006) reported a significant increase in TEP concentrations, accompanied by a decrease in Cu and Cd ligands, indicating a transformation of dissolved organic ligands (mainly polysaccharides) into colloidal/ particulate matter induced by the TEP formation mechanism. The observed lack of correlation between metal ligand concentrations and neither TOC nor Chl$a$, reported as well by Zitoun et al. (2021), is attributed to the fact that only a small fraction of the bulk TOC pool, consisting mainly of exopolysaccharides and humic-like substances, relates to metal complexing capacity (Ćosović, 2005).

A positive linear correlation was calculated for L_{Cu} and Dino <20 μm (r = 0.53, p = 0.033, n = 16) and for L_{Cd} and diatoms (0.56, 0.025, 16), indicating the release of metal ligands from specific phytoplanktonic species. The Dino genera *Gymnodinium*, *Protoperidinium*, *Tripos*, *Gyrodinium*, *Karenia*,

Scrippsiella, *Prorocentrum*, and *Alexandrium* represented 83.8% of total genera in the samples examined. Regarding diatom genera, the most abundant were *Chaetoceros* (35.1%) and *Leptocylindrus* (15.2%), followed by *Cylindrotheca* and *Pseudo-nitzschia* (approximately 14% each), with the rest of the genera detected at frequencies lower than 5% (Figure 8). Marine phytoplankton constitutes a significant source of copper ligands (Thompson et al., 2014; Nixon et al., 2019), with the fluctuations of ligand concentrations observed close to the sea surface being associated with phytoplankton ecology alterations (Nixon et al., 2021). *Emiliania huxleyi* coccolithophore produces a combination of low concentrations of strong Cu ligands with high concentrations of weak Cu ligands (Leal et al., 1999; Croot et al., 2000; Echeveste et al., 2018) and *Thalassiosira weissflogii* diatom phytochelatins as Cd complexing agents (Lee et al., 1996). On the contrary, Levy et al. (2007) demonstrated the absence of any relationship between Cu sensitivity and phytoplankton taxonomic classes, while Peña et al. (2019) noted the lack of any significant correlation between Cu ligand concentrations and diatoms or Dino abundance. The identification of specific species of phytoplankton, which are sources of metal ligands, is associated with laboratory
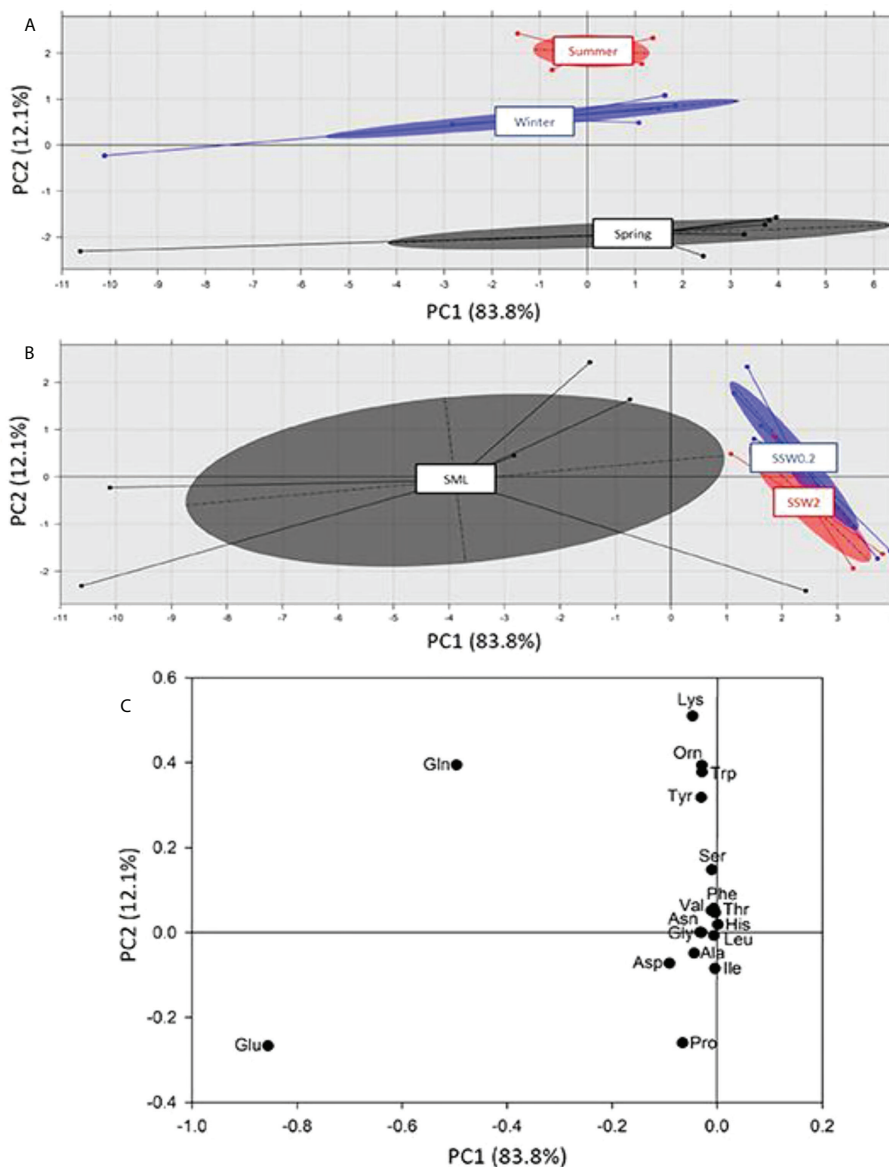
FIGURE 7
Principal component analysis of free amino acids (FAAs) content and separation on the basis of **(A)** sampling season, and **(B)** sampling depth. In **(C)** the loadings of PC2 across of which the separation is taking place are presented.

experiments involving cultures of individual phytoplankton species. In field studies, which are not characterized by the simplicity of laboratory experiments, a number of factors (abiotic sources of ligands, rapid transformation of fresh organic matter, coexistence of many different species of phytoplankton species, etc.) mask the correlations between phytoplankton and metal ligand concentrations.

The low Cu ligands concentrations (22 – 29 nM) at all depths measured during spring at Pahi of Megara site (however

not at Loutropyrgos), combined with low amino acid concentrations in POM, urge the direct investigation in the field of whether significant phytoplankton species relate with Cu ligand concentrations. Simultaneously with the decrease in Cu ligands, low abundance of bacteria, ciliates, and specific genera of Dino was recorded at Pahi station (Table 3; Figure 8) in comparison with Loutropyrgos station, where no decrease of Cu ligands was observed. Among ciliates, low abundance of *Lohmanniellidae* and *Scuticociliates* families was reported in

Pahi, while among Dino low abundance of *Gymnodinium* genera (Figure 8). ATR-FTIR spectra during spring at Pahi station revealed an intense aliphatic nature of POM particles and a lower carbohydrate content (Figure 3), pointing to the release of specific Cu ligands by specific Dino and ciliate species. Robinson and Brown (1991) have measured significant amounts of Cu ligands during an extended bloom of *Gymnodinium sanguineum* Dino and a linear increase of Cu ion complexing capacity as a function of cell density of *G. sanguineum*. Croot et al. (2000) have found that the marine Dino *Amphidinium carterae* produces very strong Cu ligands. In indoor experiments, Le Jeune et al. (2007) showed that the ciliate biomass was significantly reduced with increasing Cu concentrations, whereas the heterotrophic bacterioplankton and flagellates were not directly affected by Cu treatment in terms of biomass or diversity. Our study confirms the production of Cu ligands by Dino, more specifically *Gymnodinium* genera, pointing to their significance at coastal areas.

The lack of agreement among the highest values of Cu, Zn, and Cd L concentrations implies the occurrence of metal-specific ligands. Bruland et al. (1991) supported that single and multiple ligand classes exist in seawater, being largely metal-specific. Wells et al. (1998) demonstrated that natural organic ligands complexing Cu, Zn, Cd, and Pb in Narragansett Bay have broadly different architectures. On the contrary, studies employing linear free energy relationship (LFER) techniques for metal complexation indicated that the strongest ligand reacting with Cu, Zn, Fe, Th, and others in seawater is chemically similar to diethylenetrinitrilopenta-acetic acid (DTPA) (Hirose, 2007). In coastal environments, allochthonous sources of metal ligands affect both the amount of metal ligands and their specificity.

Toxicity of metals

At Loutropyrgos SML in spring and summer, Zn ligand concentrations are almost equal to dissolved Zn ones, indicating an incomplete Zn complexation and a subsequent increase of Zn labile fraction and its potential toxicity. The ratio of average Cu ligand concentration to Cu concentration being 6.0 in SML and 12.5 and 10.4 in $SSW_{0.2}$ and SSW_2, respectively, points to total Cu complexation, even in cases with significant variations (increases) of its concentration. The ratio of average L_{Cd} to average C_{Cd} was calculated as 10.4, 13.8, and 18.6 in SML, $SSW_{0.2}$, and SSW_2, respectively, demonstrating a strong regulation of available ligands over Cd complexation.

The European Directive 2013/39/EU (amending Directives 2000/60/EC and 2008/105/EC) sets in the field of water policy Environmental Quality Standards (EQS) of priority substances in the dissolved fraction. For "other" surface waters, referring to coastal and transitional ones, the annual average concentration (AA) for Cd is set at 17.8 nM, while the maximum allowance

concentration (MAC) is set at 13.3 nM. Dissolved Cd levels reported in the present work are lower than the specific limits. Regarding Cu and Zn, characterized as "specific pollutants," the Water Framework Directive does not establish EQS for other waters, which must be set at the national level. However, on the basis of the EU Risk Assessment Report (RAR) issued for Zn (ECI, 2008), an initial Predicted No Effect Concentration (PNEC) was proposed at 119 nM for Zn in fresh waters applied also to saline waters, revised afterward to 52 nM for saline waters (WFD-UKTAG, 2012). The latest is exceeded in the summer SML sample from Loutropyrgos site. Regarding Cu, based on the "total risk approach" employing an assessment factor (AF) and on Cu bioavailability in the presence of natural organic matter (EC, 2008), a PNEC equal to 40.9 nM for marine waters was calculated, not exceeded by the Cu values measured herewith. A toxic effect of dissolved Zn on the SML of the study area is possible, but not of Cu and Cd, confirming the findings derived from the speciation study of the specific trace metals.

Conclusions

A depletion of the SML of coastal areas in Zn binding ligands was demonstrated. The incomplete Zn complexation with organic matter is expected to provoke a significant percentage of labile Zn in SML, accompanied by a potential toxic impact, which is confirmed by comparison with PNEC values for saline waters. This is not the case for Cu and Cd, since the concentrations of their available ligands considerably exceed metal levels, fully regulating their complexation. The importance of applying methods, which enable the determination of metal ion speciation, is obvious. This is principal for drawing safe conclusions on metal bioavailability and toxicity. The simultaneous speciation study of several metal ions (such as Cu, Cd, and Zn herewith) offers the possibility of concluding on the ligand types and binding groups available/present, depending on the metal preference of binding to certain groups.

ATR-FTIR spectra, analysis of FAAs, fatty acids, and sterols, as well as calculation of SAS-to-TOC ratios, revealed a differentiation between SML and subsurface waters, relatively with the qualitative features of organic matter present. Apparently, SML organic matter is characterized as less hydrophilic and depleted of more labile components, subjected to more intense UV irradiation and bacterial activity. Metal ligand sources include both phytoplankton-derived substances and more inert organics produced during the quite rapid transformation of freshly produced organic material. It was shown that the dominant ligands in SML could be of biological origin; however, ligands of terrestrial origin could also prevail, depending on season and space.

As demonstrated also in other studies, the SML constitutes a particularly complex "ecosystem," significantly
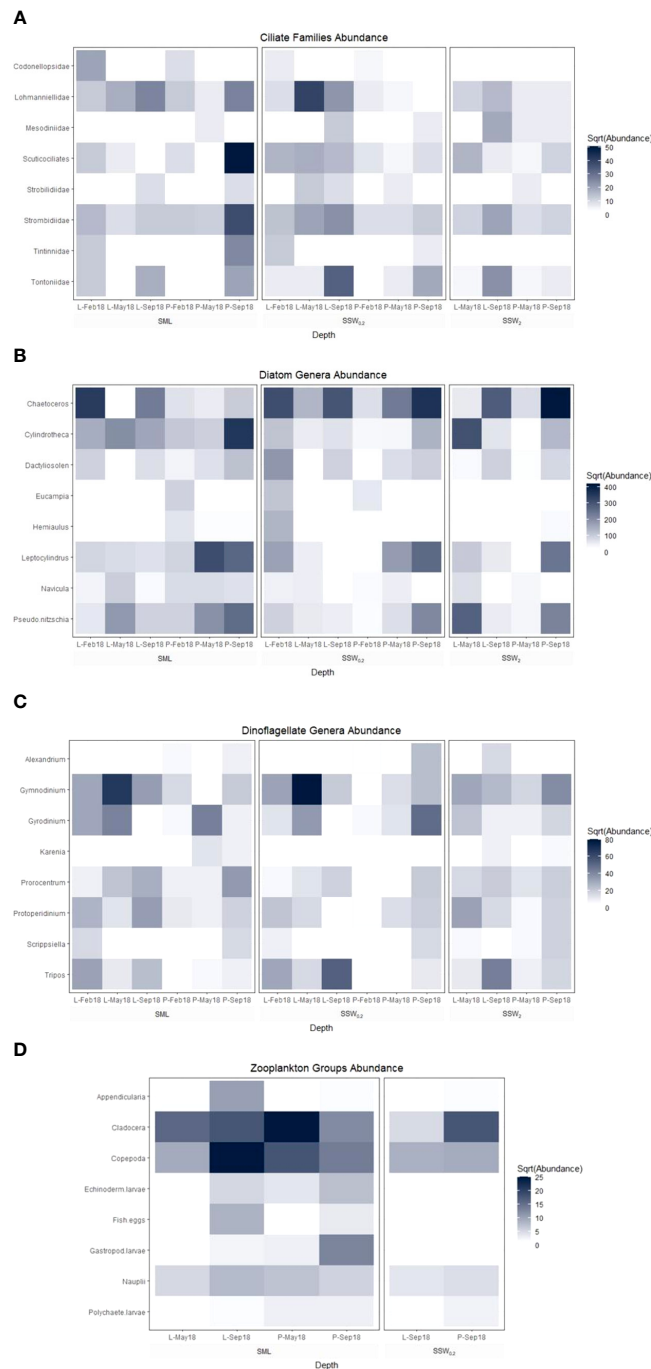
FIGURE 8
ATR-FTIR spectra of **(A)** all SML water samples collected from both sites and their comparison according to the sampling period, i.e., during **(B)** winter, **(C)** spring, and **(D)** summer.

differing from but simultaneously interacting with subsurface water. Due to both increased trace metal concentrations and qualitative differentiation of organic matter, the speciation of trace metals in SML, as in all interfaces, is of particular interest. Since studies referring to trace metal speciation in SML are limited, focusing exclusively on Cu, a considerable lack of data on bioessential elements, e.g., Fe, Zn, Co, and Cd, exists. Relevant studies may contribute to a better knowledge on the biogeochemical cycles of trace elements in surface waters.

Data availability statement

The original contributions presented in the study are included in the article/Supplementary Material. Further inquiries can be directed to the corresponding authors.

Author contributions

All authors had a significant contribution to writing the manuscript. SK, AS and MP performed metal and speciation analysis, GB ATR-FTIR analysis, DT and NK aminoacids, fatty acids and sterols analysis, AT, AG and SZ bacteria and plankton measurements. SK and AS contributed to conception, design and samplings of the study. GB performed the statistical analysis. All authors contributed to the article and approved the submitted version.

Acknowledgments

The authors would like to thank the reviewers for their constructive comments.

Conflict of interest

The authors declare that the research was conducted in the absence of any commercial or financial relationships that could be construed as a potential conflict of interest.

Publisher's note

All claims expressed in this article are solely those of the authors and do not necessarily represent those of their affiliated organizations, or those of the publisher, the editors and the reviewers. Any product that may be evaluated in this article, or claim that may be made by its manufacturer, is not guaranteed or endorsed by the publisher.

Supplementary material

The Supplementary Material for this article can be found online at: https://www.frontiersin.org/articles/10.3389/fmars.2022.932446/full#supplementary-material

References

Alsalahi, M. A., Latif, M. T., Ali, M. M., Dominick, D., Khan, M. F., Mustaffa, N. I. H., et al. (2015). Sterols as biomarkers in the surface microlayer of the estuarine areas. *Mar. pollut. Bull.* 93, 278–283. doi: 10.1016/j.marpolbul.2015.01.011

Andrew, R., Biessinger, K., and Glass, G. (1977). Effects of inorganic complexing on the toxicity of copper to daphnia magna. *Water Res.* 11, 309–315. doi: 10.1016/0043-1354(77)90064-1

Brinis, A., Mejanelle, L., Momzikoff, A., Gondry, G., Fillaux, J., Point, V., et al. (2004). Phospholipid ester-linked fatty acids composition of size-fractionated particles at the top ocean surface. *Org. Geochem.* 35, 1275–1287. doi: 10.1016/j.orggeochem.2004.04.009

Bruland, K. W. (1989). Complexation of zinc by natural organic-ligands in the central north pacific. *Limnol. Oceanogr.* 34, 269–285. doi: 10.4319/lo.1989.34.2.0269

Bruland, K. W. (1992). Complexation of cadmium by natural organic ligands in the central north pacific. *Limnol. Oceanogr.* 37, 1008–1016. doi: 10.4319/lo.1992.37.5.1008

Bruland, K. W., Donat, J. R., and Hutchins, D. A. (1991). Interactive influences of bioactive trace metals on biological production in oceanic waters. *Limnol. Oceanogr.* 36, 1555–1577. doi: 10.4319/lo.1991.36.8.1555

Bundy, R. M., Boiteau, R. M., McLean, C., Turk-Kubo, K. A., McIlvin, M. R., Saito, M. A., et al. (2018). Distinct siderophores contribute to iron cycling in the mesopelagic at station ALOHA. *Front. Mar. Sci.* 5. doi: 10.3389/fmars.2018.00061

Ćosović, B. (2005). "Surface-active properties of the sea surface microlayer and consequences for pollution in the Mediterranean Sea," in *The Mediterranean Sea, vol. 5 part K of the handbook of environmental chemistry* (Berlin/Heidelberg: Springer). doi: 10.1007/b107150

Ćosović, B., and Vojvodić, V. (1998). Voltammetric analysis of surface active substances in natural waters. *Electroanalysis* 10, 429–434. doi: 1040-0397/98/0605-0429 doi: 10.1002/(SICI)1521-4109(199805)10:6<429::AID-ELAN429>3.0.CO;2-7

Ćosović, B., Žutić, V., Vojvodić, V., and Pleše, T. (1985). Determination of surfactant activity and anionic detergents in seawater and sea surface microlayers in the Mediterranean. *Mar. Chem.* 17, 127–139. doi: 10.1016/0304-4203(85)90069-6

Cavagna, A. J., Dehairs, F., Bouillon, S., Woule-Ebongué, V., Planchon, F., Delille, B., et al. (2013). Water column distribution and carbon isotopic signal of cholesterol, brassicasterol and particulate organic carbon in the Atlantic sector of the southern ocean. *Biogeosciences* 10, 2787–2801. doi: 10.5194/bg-10-2787-2013

Chen, X. R., Gong, H. D., and Liu, C. Y. (2006). Copper complexing capacities of seawater in surface microlayer in jiaozhou bay. *HuanjingKexue/Environmental. Sci.* 27 (5), 885–891.

Chen, Y., Yang, G. P., Wu, G. W., Gao, X. C., and Xi, Q. Y. (2013). Concentration and characterization of dissolved organic matter in the surface microlayer and subsurface water of the bohai Sea, China. *Cont. Shelf. Res.* 52, 97–107. doi: 10.1016/j.csr.2012.11.007

Croot, P. L., Moffett, J. W., and Brand, L. E. (2000). Production of extracellular Cu complexing ligands by eucaryotic phytoplankton in response to Cu stress. *Limnol. Oceanogr.* 45, 619–627. doi: 10.4319/lo.2000.45.3.0619

Cunliffe, M., Engel, A., Frka, S., Gasparovic, B., Guitart, C., Murell, C., et al. (2013). Sea Surface microlayers: a unified physicochemical and biological perspective of the air–ocean interface. *Prog. Oceanogr.* 109, 104–116. doi: 10.1016/j.pocean.2012.08.004

Dachs, J., Bayona, J. M., Fowler, S. W., Miquel, J. C., and Albaigés, J. (1998). Evidence for cyanobacterial inputs and heterotrophic alteration of lipids in sinking particles in the alboran Sea (SW Mediterranean). *Mar. Chem.* 60, 179–201. doi: 10.1016/S0304-4203(97)00105-9

Danielsson, L. G., Magnusson, B., Westerlund, S., and Zhang, K. (1982). Trace metal determinations in estuarine waters by electrothermal atomic absorption spectrometry after extraction of dithiocarbamate complexes into freon. *Anal. Chim. Acta* 144, 183–188. doi: 10.1016/S0003-2670(01)95531-X

Davies, P., Goettl, J., Sinley, J., and Smith, N. (1976). Acute and chronic toxicity of lead to rainbow trout *Salmo gairdneri*, in hard and soft water. *Water Res.* 10, 199–206. doi: 10.1016/0043-1354(76)90128-7

Davison, W. (1978). Defining the electroanalytically measured species in a natural water sample. *J. Electroanal. Chem.* 87l, 395–404. doi: 10.1016/S0022-0728(78)80162-4

EC (2008). *European Union risk assessment report on zinc, the Netherlands, final report may 2008. prepared by the Netherlands organization for applied scientific research (TNO) and the national institute of public health and environment (RIVM) on behalf of the European union.*

Echeveste, P., Croot, P., and von Dassow, P. (2018). Differences in the sensitivity to Cu and ligand production of coastal vs offshore strains of emilianiahuxleyi. *Sci. Total. Environ.* 625, 1673–1680. doi: 10.1016/j.scitotenv.2017.10.050

ECI (2008). *European Union risk assessment report. voluntary risk assessment of copper, copper II sulphate pentahydrate, Copper(I) oxide, Copper(II) oxide, dicopper chloride trihydroxide. European copper institute (ECI). final version June 2008. review country* (Italy).

Elmore, S. J., Koutsidis, G., Dodson, A. T., Mottram, D. S., and Wedzicha, B. L. (2005). Measurement of acrylamide and its precursors in potato, wheat, and rye model systems. *J. Agric. Food Chem.* 53 (4), 1286–1293. doi: 10.1021/jf048557b

Engel, A., Bange, H. W., Cunliffe, M., Burrows, S. M., Friedrichs, G., Galgani, L., et al. (2017). The ocean's vital skin: Toward an integrated understanding of the sea surface microlayer. *Front. Mar. Sci.* 4. doi: 10.3389/fmars.2017.00165

Frena, M., Souza, M. R. R., Damasceno, F. C., Madureira, L. A. S., and Alexandre, M. R. (2016). Evaluation of anthropogenic contamination using sterol markers in a tropical estuarine system of northeast Brazil. *Mar. pollut. Bull.* 109, 619–623. doi: 10.1016/j.marpolbul.2016.05.022

Gachter, R., and Mares, A. (1979). MELIMEX, an experimental heavy metal pollution study: Effects of increased heavy metal loads on phytoplankton communities. *Schweiz. Z. Hydrol.* 41, 228–246. doi: 10.1007/BF02502247

Galeron, M. A., Amiraux, R., Charriere, B., Radakovitch, O., Raimbault, P., Garcia, N., et al. (2015). Seasonal survey of the composition and degradation state of particulate organic matter in the rhône river using lipid tracers. *Biogeosciences* 12, 1431–1446. doi: 10.5194/bg-12-1431-2015

Gašparović, B., Plavšić, M., Ćosović, B., and Saliot, A. (2007). Organic matter characterization in the sea surface microlayers in the subarctic Norwegian fjords region. *Mar. Chem.* 105, 1–14. doi: 10.1016/j.marchem.2006.12.010

Gledhill, M., and Buck, K. (2012). The organic complexation of iron in the marine environment: a review. *Front. Microbio.* 3. doi: 10.3389/fmicb.2012.00069

Gledhill, M., McCormack, P., Ussher, S. J., Achterberg, E. P., Mantoura, R. C., and Worsfold, P. J. (2004). Production of siderophore type chelates by mixed bacterioplankton populations in nutrient enriched seawater incubations. *Mar. Chem.* 88 (1–2), 75–83. doi: 10.1016/j.marchem.2004.03.003

Gledhill, M., Zhu, K., Rusiecka, D., and Achterberg, E. P. (2022). Competitive interactions between microbial siderophores and humic-like binding sites in European shelf Sea waters. *Front. Mar. Sci.* 9. doi: 10.3389/fmars.2022.855009

Gordon, A. S., Dyer, B. J., Kango, R. A., and Donat, J. R. (1996). Copper ligands isolated from estuarine water by immobilized metal affinity chromatography: temporal variability and partial characterization. *Mar. Chem.* 53, 163–I72. doi: 10.1016/0304-4203(96)00022-9

Goutx, M., and Saliot, A. (1980). Relationship between dissolved and particulate fatty acids and hydrocarbons, chlorophyll a and zooplankton biomass in villefranche bay, Mediterranean Sea. *Mar. Chem.* 8, 299–318. doi: 10.1016/0304-4203(80)90019-5

Hardy, J. T. (1982). The sea surface microlayer: Biology, chemistry and anthropogenic enrichment. *Prog. Oceanogr.* 11, 307–328. doi: 10.1016/0079-6611(82)90001-5

Hardy, J. T. (1997). "Biological effects of chemicals in the sea-surface microlayer," in *The seasurface and global change*. Eds. P. S. Liss and R. A. Duce (Cambridge, England:Cambridge University Press), 339–370.

Hart, B. (1981). Trace metal complexing capacity of natural waters: A review. *Environ. Techn.* 2, 95. doi: 10.1080/09593338109384029

Harvey, G. W., and Burzell, L. A. (1972). A simple microlayer method for small samples. *Limnol. Oceanogr.* 17, 156–157. doi: 10.4319/lo.1972.17.1.0156

Hirose, K. (2007). Metal–organic matter interaction: Ecological roles of ligands in oceanic DOM. *Appl. Geochem.* 22 (8), 1636–1645. doi: 10.1016/j.apgeochem.2007.03.042

Holm-Hansen, O., Lorenzen, C. J., Holmes, R. W., and Strickland, J. D. H. (1965). Fluorometric determination of chlorophyll. *ICES. J. Mar. Sci.* 30 (1), 3–15. doi: 10.1093/icesjms/30.1.3

How, Z. T., Busetti, F., Linge, K. L., Kristiana, I., Joll, C. A., and Charrois, J. W. A. (2014). Analysis of free amino acids in natural waters by liquid chromatography-tandem mass spectrometry. *J. Chromatogr. A.* 1370, 135–146. doi: 10.1016/j.chroma.2014.10.040

Jakuba, R. W., Saito, M. A., Moffett, J. W., and Xu, Y. (2012). Dissolved zinc in the subarctic north pacific and Bering Sea: Its distribution, speciation, and importance to primary producers. *Global Biogeochem. Cycles.* 26, GB2015. doi: 10.1029/2010GB004004

Karavoltsos, S., Kalambokis, E., Sakellari, A., Plavsic, M., Dotsika, E., Karalis, P., et al. (2015). Organic matter characterization and copper complexing capacity in the sea surface microlayer of coastal areas of the Eastern Mediterranean. *Mar. Chem.* 173, 234–243. doi: 10.1016/j.marchem.2014.12.004

Karavoltsos, S., Sakellari, A., Dassenakis, M., Bakeas, E., and Scoullos, M. (2021). Trace metals in the marine surface microlayer of coastal areas in the Aegean sea,

Eastern Mediterranean. *Estuar. Coast. Shelf. Sci.* 259, 107462. doi: 10.1016/j.ecss.2021.107462

Kim, J.-M., Baars, O., and Morel, F. M. M. (2016). The effect of acidification on the bioavailability and electrochemical lability of zinc in seawater. *Phil. Trans. R. Soc A.* 374, 20150296. doi: 10.1098/rsta.2015.0296

Kim, T., Obata, H., and Gamo, T. (2015b). Dissolved zn and its speciation in the northeastern Indian ocean and the Andaman Sea. *Front. Mar. Sci.* 2. doi: 10.3389/fmars.2015.00060

Kim, T., Obata, H., Kondo, Y., Ogawa, H., and Gamo, T. (2015a). Distribution and speciation of dissolved zinc in the western north pacific and its adjacent seas. *Mar. Chem.* 173, 330–341. doi: 10.1016/j.marchem.2014.10.016

Kuznetsova, M., and Lee, C. (2002). Dissolved free and combined amino acids in nearshore seawater, sea surface microlayers and foams: Influence of extracellular hydrolysis. *Aquat. Sci.* 64, 252–268. doi: 10.1007/s00027-002-8070-0

Kuznetsova, M., Lee, C., Aller, J., and Frew, N. (2004). Enrichment of amino acids in the sea surface microlayer at coastal and open ocean sites in the north Atlantic ocean. *Limnol. Oceanogr.* 49 (5), 1605–1619. doi: 10.4319/lo.2004.49.5.1605

Laglera, L. M., and van den Berg, C. M. G. (2003). Copper complexation by thiol compounds in estuarine waters. *Mar. Chem.* 82, 71–89. doi: 10.1016/S0304-4203(03)00053-7

Leal, M. F. C., Vasconcelos, M. T. S. D., and van Den Berg, C. M. G. (1999). Copper-induced release of complexing ligands similar to thiols by *Emiliania huxleyi* in seawater cultures. *Limnol. Oceanogr.* 44, 1750–1762. doi: 10.4319/lo.1999.44.7.1750

Lee, J. G., Ahner, B. A., and Morel, M. M. (1996). Export of cadmium and phytochelatin by the marine diatom *Thalassiosira weissflogii*. *Environ. Sci. Technol.* 30, 1814–1182. doi: 10.1021/es950331p

Lee, J. G., Roberts, B. S., and Morel, F. M. M. (1995). Cadmium: A nutrient for the marine diatom *Thalassiosira weissflogii*. *Limnol. Oceanogr.* 40 (6), 1056–1063. doi: 10.4319/lo.1995.40.6.1056

Le Jeune, A.-H., Charpin, M., Sargos, D., Lenain, J.-F., Deluchat, V., Ngayila, N., et al. (2007). Planktonic microbial community responses to added copper. *Aquat. Toxicol.* 83, 223–237. doi: 10.1016/j.aquatox.2007.04.007

Levy, J. L., Stauber, J. L., and Jolley, D. F. (2007). Sensitivity of marine microalgae to copper: the effect of biotic factors on copper adsorption and toxicity. *Sci. Total. Environ.* 387, 141–154. doi: 10.1016/j.scitotenv.2007.07.016

Liss, P. S., and Duce, R. A. (1997). The Sea surface and global change. *Cambridge. Univ. Press.* 1–519. doi: 10.1017/CBO9780511525025

Lorenzo, J. I., Beiras, R., Mubiana, V. K., and Blust, R. (2005). Copper uptake by mytilus edulis in the presence of humic acids. *Environ. Toxicol. Chem.* 24 (4), 973–980. doi: 10.1897/04-216r.1

Morel, F. (2008). The co-evolution of phytoplankton and trace element cycles in the oceans. *Geobiology* 6, 318–324. doi: 10.1111/j.1472-4669.2008.00144.x

Mühlebach, A., Albers, C., and Kattner, G. (1999). Differences in the sterol composition of dominant Antarctic zooplankton. *Lipids* 34, 45–51. doi: 10.1007/s11745-999-336-1

Muller, F. L. L., and Kester, D. R. (1991). Voltammetric determination of the complexation parameters of zinc in marine and estuarine waters. *Mar. Chem.* 33, 71–90. doi: 10.1016/0304-4203(91)90058-5

Nixon, R. L., Jackson, S. L., Cullen, J. T., and Ross, A. R. S. (2019). Distribution of copper-complexing ligands in Canadian Arctic waters as determined by immobilized copper(II)-ion affinity chromatography. *Mar. Chem.* 215, 103673. doi: 10.1016/j.marchem.2019.103673

Nixon, R. L., Peña, M. A., Taves, R., Janssen, D. J., Cullen, J. T., and Ross, A. R. S. (2021). Evidence for the production of copper-complexing ligands by marine phytoplankton in the subarctic northeast pacific. *Mar. Chem.* 237, 104034. doi: 10.1016/j.marchem.2021.104034

Noble, A. E., Ohnemus, D. C., Hawco, N. J., and Lam, P. J. (2017). Coastal sources, sinks and strong organic complexation of dissolved cobalt within the US north Atlantic GEOTRACES transect GA03. *Biogeosciences* 14, 2715–2739. doi: 10.5194/bg-14-2715-2017

Passow, U. (2002). Transparent exopolymer particles (TEP) in aquatic environments. *Prog. Oceanogr.* 55, 287–333. doi: 10.1016/S0079-6611(02)00138-6

Passow, U., and Alldredge, A. L. (1995). A dye-binding assay for the spectrophotometric measurement of transparent exopolymer particles (TEP). *Limnol. Oceanogr.* 40, 1326–1335. doi: 10.4319/lo.1995.40.7.1326

Peña, M. A., Nemcek, N., and Robert, M. (2019). Phytoplankton responses to the 2014–2016 warming anomaly in the northeast subarctic pacific ocean. *Limnol. Oceanogr.* 64, 515–525. doi: 10.1002/lno.11056

Peng, X., Zhang, G., Mai, B., Hu, J., Li, K., and Wang, Z. (2005). Tracing anthropogenic contamination in the pearl river estuarine and marine environment of south China Sea using sterols and other organic molecular markers. *Mar. pollut. Bull.* 50, 856–865. doi: 10.1016/j.marpolbul.2005.02.031

Plavšić, M., Gašparović, B., and Ćosović, B. (2007). Copper complexation and surfactant activity of organic matter in coastal seawater and surface microlayer samples from north Norwegian fjords and NW Mediterranean region. *Fresenius. Environ. Bull.* 16 (4), 372–378.

Plavšić, M., Krznarić, D., and Branica, M. (1982). Determination of the apparent copper complexing capacity of seawater by DPASV. *Mar. Chem.* 11, 17–31. doi: 10.1016/0304-4203(82)90045-7

Porter, K. G., and Feig, Y. S. (1980). The use of DAPI for identifying and counting aquatic microflora. *Limnol. Oceanogr.* 25 (5), 943–948. doi: 10.4319/lo.1980.25.5.0943

Posacka, A. M., Semeniuk, D. M., and Maldonado, M. T. (2019). Effects of copper availability on the physiology of marine heterotrophic bacteria. *Front. Mar. Sci.* 5. doi: 10.3389/fmars.2018.00523

Prifti, E., Kaberi, H., Paraskevopoulou, V., Michalopoulos, P., Zeri, C., Iliakis, S., et al. (2022). Vertical distribution and chemical fractionation of heavy metals in dated sediment cores from the saronikos gulf, Greece. *J. Mar. Sci. Eng.* 10, 376. doi: 10.3390/jmse10030376

Robinson, M. G., and Brown, L. N. (1991). Copper complexation during a bloom of *Gymnodinium sanguineum* hirasaka (Dinophyceae) measured by ASV. *Mar. Chem.* 33, 105–118. doi: 10.+1016/0304-4203(91)90060-A

Ružící, I. (1982). Theoretical aspects of the direct titration of natural waters and its information yield for trace metal speciation. *Anal. Chim. Acta* 140, 99–113. doi: 10.1016/S0003-2670(01)95456-X

Sakellari, A. (2006). *Biogeochemical study of metals: Study of trace elements cycle in seawater and sediment and investigation of their impact on the food chain. PhD thesis (in Greek).*

Sakellari, A., Plavšić, M., Karavoltsos, S., Dassenakis, M., and Scoullos, M. (2011). Assessment of copper, cadmium and zinc remobilization in Mediterranean marine coastal sediments. *Estuar. Coast. Shelf. Sci.* 91, 1–12. doi: 10.1016/j.ecss.2010.09.008

Saliot, A., Marty, J. C., Scribe, P., Sicre, M. A., Viets, T. C., De leeuw, J. W., et al. (1991). Characterization of particulate organic matter in Mediterranean sea-surface films and underlying water by flash pyrolysis and gas chromatographic analyses. *Org. Geochem.* 17, 329–340. doi: 10.1016/0146-6380(91)90096-3

Santos-Echeandía, J., Laglera, L. M., Prego, R., and van den Berg, C. M. G. (2008). Copper speciation in estuarine waters by forward and reverse titrations. *Mar. Chem.* 108, 148–158. doi: 10.1016/j.marchem.2007.11.004

Santos-Echeandia, J., Prego, R., Cobelo- García, A., and Millward, G. E. (2009). Porewater geochemistry in a Galician ria (NW Iberian peninsula): Implications for benthic fluxes of dissolved trace elements (Co, Cu, Ni, Pb, V, zn). *Mar. Chem.* 117, 77–87. doi: 10.1016/j.marchem.2009.05.001

Scoullos, M. (1986). Lead in coastal sediments: The case of the elefsis gulf, Greece. *Sci. Total. Environ.* 49, 199–219. doi: 10.1016/0048-9697(86)90240-8

Scoullos, M., Plavšić, M., Karavoltsos, S., and Sakellari, A. (2006). Partitioning and distribution of dissolved copper, cadmium and organic matter in Mediterranean marine coastal areas: The case of a mucilage event. *Estuar. Coast. Shelf. Sci.* 67, 484–490. doi: 10.1016/j.ecss.2005.12.007

Socrates, G. (2001). *Infrared and raman characteristic group frequencies: Tables and charts* (Chichester, UK: John Wiley and Sons Inc), ISBN: .

Sunda, W. G., and Huntsman, S. A. (1995). Cobalt and zinc interreplacement in marine phytoplankton: biological and geochemical implications. *Limnol. Oceanogr.* 40, 1404–1417. doi: 10.2307/2838496

Sunda, W. G., and Huntsman, S. A. (1998). Interactions among Cu^{2+}, Zn^{2+}, and Mn^{2+} in controlling cellular Mn, zn, and growth rate in the coastal alga *Chlamydomonas*. *Limnol. Oceanogr.* 43, 1055–1064. doi: 10.4319/lo.1998.43.6.1055

Tada, K., Tada, M., and Maita, Y. (1998). Dissolved free amino acids in coastal seawater using a modified fluorometric method. *J. Oceanogr.* 54, 313–321. doi: 10.1007/BF02742615

Thompson, C. M., Ellwood, M. J., and Sander, S. G. (2014). Dissolved copper speciation in the Tasman Sea, SW pacific ocean. *Mar. Chem.* 164, 84–94. doi: 10.1016/j.marchem.2014.06.003

Tovar-Sánchez, A., Arrieta, J. M., Duarte, C. M., and Sañudo-Wilhelmy, S. A. (2014). Spatial gradients in trace metal concentrations in the surface microlayer of the Mediterranean Sea. *Front. Mar. Sci.* 1, 79. doi: 10.3389/fmars.2014.00079

Tovar-Sánchez, A., Rodríguez-Romero, A., Engel, A., Zäncker, B., Fu, F., Marañón, E., et al. (2020). Characterizing the surface microlayer in the Mediterranean Sea: trace metal concentrations and microbial plankton abundance. *Biogeosciences* 17, 2349–2364. doi: 10.5194/bg-17-2349-2020

Tremblay, L., and Alaoui, G. (2011). Characterization of aquatic particles by direct FTIR analysis of filters and quantification of elemental and molecular compositions. *Environ. Sci. Technol.* 45, 9671–9679. doi: 10.1021/es202607n

Tzempelikou, E., Zeri, C., Iliakis, S., and Paraskevopoulou, V. (2021). Cd, Co, Cu, Ni, Pb, zn in coastal and transitional waters of Greece and assessment of background concentrations: Results from 6 years implementation of the water framework directive. *Sci. Total. Environ.* 774, 145177. doi: 10.1016/j.scitotenv.2021.145177

van den Berg, C. M. G. (1982). Determination of copper complexation with natural organic ligands in seawater by equilibration with MnO2: II. experimental procedures and application to surface seawater. *Mar. Chem.* 11, 323–342. doi: 10.1016/0304-4203(82)90028-7

van den Berg, C. M. G., and Donat, J. R. (1992). Determination and data evaluation of copper complexation by organic ligands in sea water using cathodic stripping voltammetry at varying detection windows. *Anal. Chim. Acta* 257, 281–291. doi: 10.1016/0003-2670(92)85181-5

Volkman, J. K. (1986). A review of sterol markers for marine and terrigenous organic matter. *Org. Geochem.* 9, 83–99. doi: 10.1016/0146-6380(86)90089-6

Volkman, J. K. (2003). Sterols in microorganisms. *Appl. Microbiol. Biotechnol.* 60, 495–506. doi: 10.1007/s00253-002-1172-8

Volkman, J. K., Barrett, S. M., Blackburn, S. I, Mansour, M. P., Sikes, E. I., and Gelin, F. (1998). Microalgal biomarkers: A review of recent research developments. *Org. Geochem.* 29, 1163–1179. doi: 10.1016/S0146-6380(98)00062-X

Vong, L., Laes, A., and Blain, S. (2007). Determination of iron–porphyrin-like complexes at nanomolar levels in seawater. *Anal. Chim. Acta* 588, 237–244. doi: 10.1016/j.aca.2007.02.007

Vraspir, J., and Butler, A. (2009). Chemistry of marine ligands and siderophores. *Ann. Rev. Mar. Sci.* 1, 43–63. doi: 10.1146/annurev.marine.010908.163712

Wells, M., Kozelka, P., and Bruland, K. (1998). The complexation of "dissolved" Cu, zn, cd and Pb by soluble and colloidal organic matter in Narragansett bay. *Mar. Chem.* 62, 203–217. doi: 10.1016/S0304-4203(98)00041-3

WFD-UKTAG (2012). *Proposed EQS for water framework directive annex VIII substances: Zinc (For consultation), water framework directive – united kingdom advisory group (WFD-UKTAG)* (Edinburgh, Scotland:Water Framework Directive - United Kingdom Technical Advisory Group (WFD-UKTAG)).

Witter, A. E., Hutchins, D. A., Butler, A., and Luther, G. W. (2000). Determination of conditional stability constants and kinetic constants for strong model fe binding ligands in seawater. *Mar. Chem.* 69, 1–17. doi: 10.1016/S0304-4203(99)00087-0

Wurl, O., Ekau, W., Landing, W. M., and Zappa, C. J. (2017). Sea Surface microlayer in a changing ocean – a perspective. *Elementa.: Sci. Anthropocene.* 5, 31. doi: 10.1525/elementa.228

Wurl, O., Miller, L., and Vagle, S. (2011). Production and fate of transparent exopolymer particles in the ocean. *J. Geophys. Res.* 116, C00H13. doi: 10.1029/2011JC007342

Yang, G. P., Chen, Y., and Gao, X. C. (2009). Distribution of dissolved free amino acids, dissolved inorganic nitrogen and chlorophyll a in the surface microlayer and subsurface water of the yellow Sea, China. *Cont. Shelf. Res.* 29 (14), 1737–1747. doi: 10.1016/j.csr.2009.05.015

Zhao, C.-M., Campbell, P. G. C., and Wilkinson, K. J. (2016). When are metal complexes bioavailable? *Environ. Chem.* 13, 425–433. doi: 10.1071/EN15205

Zitoun, R., Achterberg, E. P., Browning, T. J., Hoffmann, L. J., Krisch, S., Sander, S. G., et al. (2021). The complex provenance of Cu-binding ligands in the south-East Atlantic. *Mar. Chem.* 237, 104047. doi: 10.1016/j.marchem.2021.104047